University of Southern Queensland

Faculty of Health, Engineering and Sciences

Remote Sensed Monitoring of Seagrass Cover in the Gippsland Lakes, Victoria, Australia.

A dissertation submitted by

Conan Kuzniarski

in fulfilment of the requirements of

ENG4111 and 4112 Research Project

towards the degree of

Bachelor of Spatial Science (Honours) (Surveying)

Submitted October, 2019

Abstract

Seagrass presence in waterways across the world is an integral part of a healthy aquatic environment. Seagrass meadows provide food, shelter and protection for a large range of aquatic species, along with the filtration of water and stability of benthic environments. This work explores the application of remote sensed data to reliably determine the spatial patterns of growth and decline in seagrass meadows within the Gippsland Lakes, Victoria, Australia, in an efficient and economical way. This was done over a 20-year, bi-annual time series from 1998 to 2017 at three separate sites in Lake King and Lake Victoria. Landsat 5 and Landsat 7 pre-processed data was obtained from Geoscience Australia, where a local NBAR correction has been applied to their entire archives of Landsat data. Grass GIS and QGIS open source software was used to perform a supervised classification of three and five band combinations to determine the most statically accurate combination to then apply to the entire time series. The five-band combination of red, green, blue and two near infra-red bands, produced marginally better results of 76% total accuracy and was therefore applied to the entire time series. Each of the three study sites; Gorcrow Point, Point King and Waddy Island, showed dissimilar trends in seagrass cover, however, correlations exist with historical research. These results will provide the scope for future work to enhance the use of this method in delivering significant savings in the monitoring of seagrass meadows in shallow coastal environments.

University of Southern Queensland

Faculty of Health, Engineering and Sciences

ENG4111/ENG4112 Research Project

Limitations of Use

University of Southern Queensland

Faculty of Health, Engineering and Sciences

ENG4111/ENG4112 Research Project

Certification of Dissertation

I certify that the ideas, designs and experimental work, results, analyses and conclusions set out in this dissertation are entirely my own effort, except where otherwise indicated and acknowledged.

I further certify that the work is original and has not been previously submitted for assessment in any other course or institution, except where specifically stated.

C. Kuzniarski

[redacted]

Acknowledgements

The completion of this dissertation would not have been possible without Dr Glenn Campbell's expert insight into the formulation of a meaningful and enjoyable project. His support, guidance and advice has continued for the duration of this project and I thank him very much for it.

My biggest fans and most staunch supporters are my amazing wife Jessica and two daughters Lola and Wren, who both learnt, understood and embraced the concept of support. They have not only sacrificed considerable family time but have also had to work through the chaos with me.

This is as much their achievement as it is mine.

Table of Contents

List of Figures

List of Tables

1.0 Introduction

The Gippsland Lakes are a series of coastal lakes that encompass over 360 km^2 (Gullan, Walsh & Forbes 1981) on Victoria's south eastern coast (*see Figure 1*) and are permanently open to Bass Strait via an artificial and constantly dredged channel at Lakes Entrance and are fed by four large local rivers that encompass a catchment area of 22,000 km^2 (Gullan, Walsh & Forbes 1981). The lake system houses many seagrass meadows, located from the ocean entrance, where these areas are flushed with fresh sea waters twice daily through to areas with higher concentrations of terrestrial runoffs up to 70 kilometres away.

Figure 1.1 *Gippsland Lakes, Victoria, Australia (Gippsland Ports 2016)*

Seagrasses are an integral component to a healthy ecosystem and the monitoring of submerged coastal fringes is beneficial to environmental management and other industries such as commercial and recreational fishing (Ferguson, Korfmacher 1997). In the Gippsland Lakes, seagrass meadows are predominately found at depths between 0 – 2.5 meters and generally at less than 2 metres depth (Roob & Ball 1997 & Ferguson, Korfmacher 1997). They have an enormous impact on the health of the local water quality, by aiding in lowering suspended solids, silicate and phosphorous and stabilising sediments. Seagrass also provides food, shelter and protection to a large range of organisms, juvenile aquatic species and benthic foragers (Blake, Roob & Patterson 2000 & Lyons, Phinn & Roelfsema 2010).

Seagrass has been studied extensively across the globe due to its impact on the health of an ecosystem. Being able to present spatial patterns of growth and decline of such an import component of coastal waterways is vital in aiding ongoing management procedures by providing reference data (Lyons, et al. 2010). This outcome is enhanced by utilising a data set from 1998 to 2017, as this will offer a greater period to interpret trends of seagrass meadows (Lyons et al. 2010).

In the Gippsland Lakes, four species of seagrass have been recorded, which are Zostera muelleri, Heterozostera tasmanica, Ruppia spiralis, and Lepilaena cylindrocarpa (Roob & Ball 1997). However, this project will only be identifying a seagrass presence, regardless of species.

The desired aim of this study is to determine if a reliable, more cost-effective solution can be implemented using satellite remote sensing to that of studies which require the addition of expensive field crews and equipment. This is ascertained by calculating the most reliable processing method to monitor seagrass meadows in the Gippsland Lakes by comparing results between pixel-based, supervised classification combinations of three visible bands; Red, Green and Blue (RGB) and five bands; RGB + Near Infra-Red (NIR). The project then aims to map the spatial extent of these seagrass meadows at three locations in varying areas and conditions of the lake system. This will be done by utilising historical satellite imagery from Landsat 5, with a thematic mapper (TM) sensor and Landsat 7 with an Enhanced Thematic Mapper Plus sensor (ETM+). Using 20 years of data at generally equal biannual epochs will allow for a comprehensive analysis of change in the size and locations of the seagrass meadows within the project sites.

The importance of seagrass meadows to the ongoing health of waterways such as the Gippsland Lakes cannot be stressed enough and through efficient and cost-effective monitoring of these meadows, the hope of providing a greater understanding of the condition, cycles and relationship to environmental effects can be achieved. Traditional methods for site observations are time consuming and very costly, through the utilisation of speciality equipment and trained personnel. However, with a host of different satellites adding to vast databases of imagery daily and opensource software all available free of cost, the ability to monitor large areas accurately and efficiently is now possible. It is, therefore, this project's aim to use previously researched sites, studied in 1997 by Roob and Ball, who utilised a historical time series of aerial photography to provide a comparison and to then establish the most accurate band combination for ascertaining the spatial distribution of seagrass meadows in the Gippsland Lakes between 1998 – 2017 using remote sensing.

2.0 Literature Review

2.1 Remote Sensing

Remote sensing is the recording of an object from a distance which is done through the theory as explained in Maini (2014, p. 10101m), that each object has a '…unique characteristic reflection and emission spectra' that enables the identification of that object through image processing. Remote sensing is used by an extensive group of professionals such as, Surveyors, Biologists and agriculturalists to aid in research and monitoring of the health of crops and water resources etcetera. Multiple platforms exist for remote sensing applications; however, satellites have become the primary source (Maini 2014) with close to 600 earth observation satellites orbiting the earth as of 2017 (Pixalytics 2017).

2.1.1 Spectral Reflectance

Natural and built features on the earth's surface possess different spectral reflectance and remittance properties which can be interpreted through a process named image classification (Al-doski 2013). This allows an analyst to observe properties of an object that humans could not ordinarily perceive, as humans can only see a small section of the electromagnetic bands called the visible band which has a wavelength of $0.4 - 0.7\ \mu\text{m}$. To identify these variations in spectral responses, the analyst is required to find the ideal combination of bands and time of year to best interpret the individual signatures of the class of interest (Eastman 2001).

Table 2.1 *Shows different electromagnetic bands and their associated wavelengths, relative to remote sensing (University of Southern Queensland, 2018)*

Electromagnetic Band	Wavelength	Remarks
Gamma ray	<0.03 nm	Incoming radiation is mostly absorbed by the upperatmosphere, and is not available for earth resources remote sensing.
X-ray	0.03 to 3 nm	Incoming radiation is completely absorbed byatmosphere and hence has no remote sensing application.
Ultraviolet, UV	3 nm to 0.4 μm	<0.3 μm is completely absorbed by upper atmosphere ozone.
Photographic UV	0.3 to 0.4 μm	Detectable with film and photodetectors, but diminished through severe atmospheric scattering.
Visible	0.4 to 0.7 μm	Detected with film and photodetectors (peak at about 0.5 μm).
Infrared, IR	0.7 to 300 μm	Interaction with matter varies with wavelength.
Reflected IR	0.7 to 3 μm	Primarily reflected solar radiation and contains no information about thermal properties of materials. 0.7 to 0.9 μm radiation is detectable with *photographic IR radiation film*.
Thermal IR	3 to 5 μm 8 to 14 μm	Principal atmospheric windows in the thermal region where optical-mechanical scanners are used to acquire imagery.
Microwave	0.3 to 300 cm	Can penetrate clouds and fog and imagery is acquired inthe active or passive mode.
Radar	0.3 to 300 cm	Microwave remote sensing using the active mode.

2.1.2 Benthic Zone

The benthic zone is an ecological area within a body of water that consists of the bottom or floor, the sediment surface and some sub-surface layers. These zones occur in both fresh and salt waters, at all depths of water and are determined by distinct conditions such as biological, physical, and geochemical characteristics (New World Encyclopedia 2013). These zones are integral to the health of lake systems such as the Gippsland lakes, due to the broad species they support (Zaiko 2008).

The ability to obtain suitable results of seagrass meadows within the benthic zone through remote sensing is affected by a lack of light in the water column. This is due to scattering, where photons are deflected from their original path when they impact water and suspended particles, or are absorbed, where the light is either transformed into another type of energy such as heat or chemical potential energy (Contreras-Silva, López-Caloca, Tapia-Silva & Cerdeira-Estrada 2012). Furthermore, this affects bands differently due to different rates of attenuation, for example within the visible bands a shorter wavelength such as the blue band will attenuate at a more rapid pace than the red band (Contreras-Silva, López-Caloca, Tapia-Silva & Cerdeira-Estrada 2012).This is significant when using satellite data to identify seagrass meadows as the spectral reflectance needs to be determined in order to process and differentiate between other aquatic plants and objects. It is important to be aware that determination of the spectral reflectance of land-based plants and aquatic species if very different. This is due to the fact that water is very high in absorption and reflects almost no near infrared wavelengths (Humboldt State Geospatial Online 2014) and therefore detecting the spectral reflectance is restricted to visible wavelengths due to the radiated light penetrating the water column and reflecting to the satellite sensor, as can be seen in *Figures 2.1 and 2.2*. However, land-based plants are best observed using Near Infra-Red (0.76 – 0.9) and short infrared wave lengths (Fyfe 2003). Within the visual band the optimum results can be obtained from Landsat 5 and Landsat 7's band 1 (blue), which has a wavelength of 0.45 - 0.52 and provides the best results for bathymetric mapping of seagrasses (USGS n.d. & Van Niel, Holmes & Radford 2009).

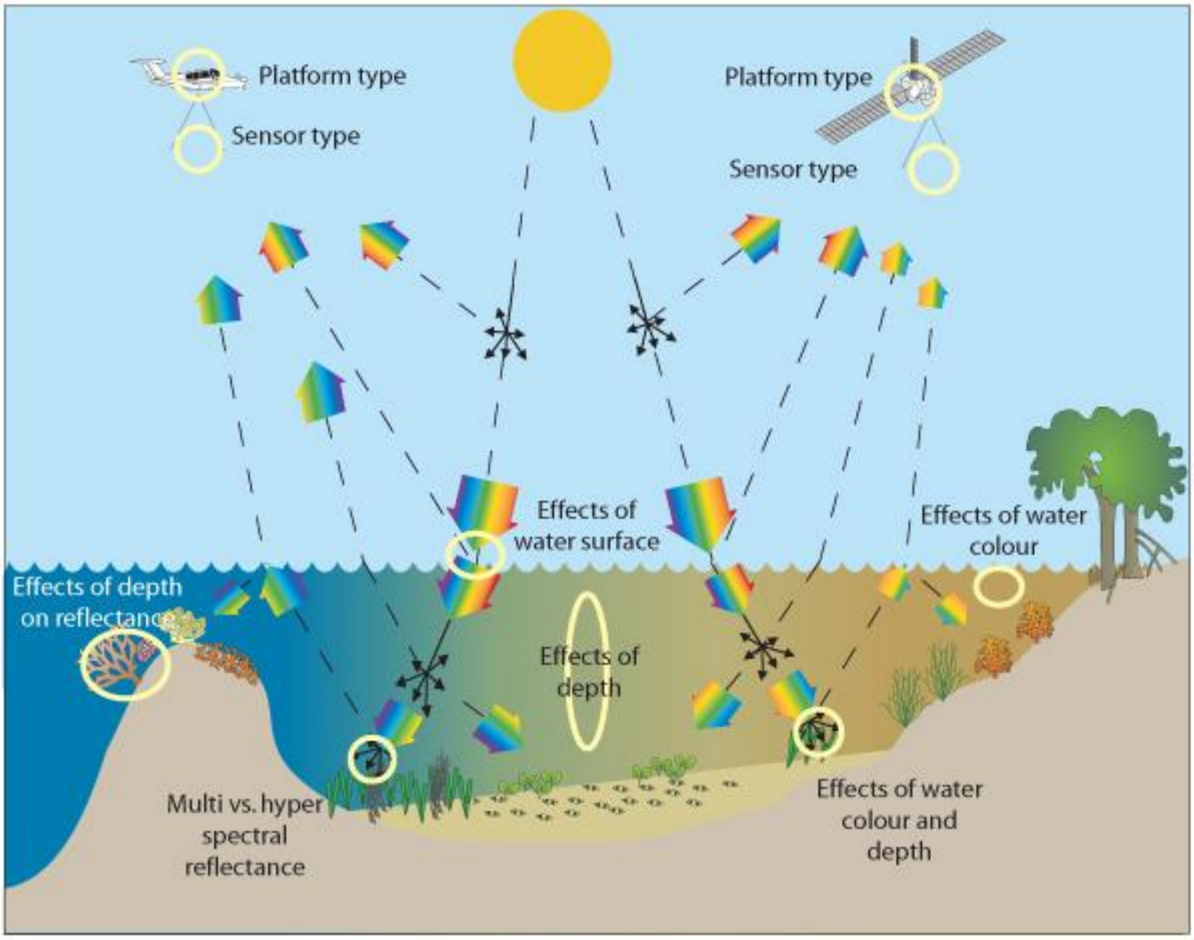

Figure 2.1 *The physical process of remote sensing and the interactions and effects on light in a passive sensor setup, such as Landsat (The University of Queensland, Australia n.d.).*

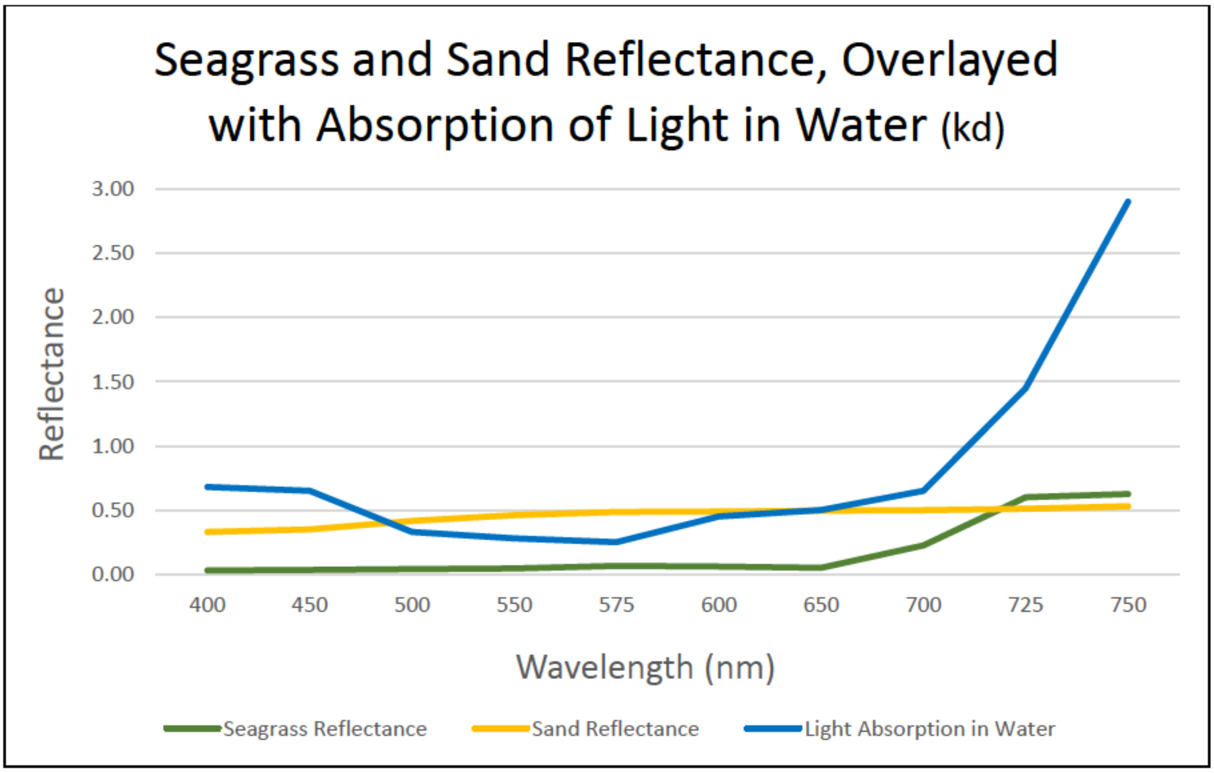

Figure 2.2 *Seagrass and sand reflectance values through the visible light bands, to the near-infra red at 700+ nm. This is overlayed with the wavelength-dependant absorption of light (Kd).*

2.2 Landsat History

The Landsat Program is a joint venture between NASA and the United States Geological Survey (USGS) and has been collecting Earth Observation (EO) data since 1972. This began with Landsat 1 and has continued through to present day with Landsat 7 and 8 being currently operational and Landsat 9 due for launch in December 2020 (Wulder et al. 2019).

In 2008 this program encountered a significant rise in the scientific investigations and applications due to the Landsat archives being made freely available to the public through the open access data policy (Landsat Data Policy) (Wulder et al. 2012). A crucial implication of this was the ability for users to monitor and map change in the earth's surface through a time series and at a more detailed perspective than ever before (Wulder et al. 2012), which has provided the scope for this dissertation to proceed.

Figure 2.3 *Time series for Landsat Satellite launch and decommission dates (United States Geological Survey n.d.).*

2.3 Pre-processed Landsat Data

Remote sensed data is not collected ready for use, the initial solar spectral range received by satellite sensors does not replicate the reflectance values of the surface objects (Li et al. 2010). The variances in these values can be attributed to differences in atmospheric properties, sun position, sensor view angle, surface slope and surface aspect and needs to be corrected to ensure the data is consistent over space and time (Kool 2017). To achieve consistent and comparable data, Geo-Science Australia (GA), have released a Surface Reflectance (SR) suite which is part of the EO product. This suite delivers a product called Surface Reflectance NBAR+ (Nadir-corrected BRDF Adjusted Reflectance, where BRDF stands for Bidirectional reflectance distribution function) (Kool 2017). The Surface Reflectance NBAR+ automated process calculates corrections for "…variations in solar illumination, the combined variations in sun and satellite view angles, the presences of aerosols and atmospheric moisture content (radiative transfer modelling), and the BRDF of the target" (Lewis et al. 2017 p. 280). The outcome provides a medium resolution (~25 m) grid, based on Landsat imagery for the continent and coastal fringes of Australia and is applied to GA's entire Landsat TM/ETM+/OLI imagery archives from 1987 to the present (Kool 2017).

The implementation of Surface Reflectance NBAR+ provides significant positives for research such as this dissertation, as the scope for accurate environmental mapping has historically been minimal due to inadequate traditional methods that have only corrected for inherent geometric and radiometric distortions (Geoscience Australia 2015). Lyons et al. (2012) have extensively studied the seagrass meadows of Moreton Bay Queensland using pre-processed data from the remote sensing centre section of Queensland Department of Environment and Resource Management (DERM). The TM and ETM+ imagery data that Lyons et al. (2013) have used has been validated radiometrically and geometrically corrected via an automated routine, which adjusts data to top of atmosphere radiance with sub pixel geometric accuracy (Danaher et al. and de Vries et al., cited in Lyons 2013), which confirms the ability of pre-processed data to provide a reliable outcome.

2.4 Accuracy Assessment

The assessment of accuracy for thematic maps became possible with the development of digital imagery, namely the creation of Landsat (Congalton 2015). Initially, accuracy assessment wasn't prevalent until the late 1980's when considerable work was done to address this component of the science. This coupled with technological advancements in spatial and spectral resolution sensors and computational algorithms, has made way for site-specific accuracy assessment which provides the ability to vigorously assess the user's output (Congalton 2015).

When implementing an error matrix there are two elements that should be considered: classification scheme and sources of error. The classification scheme component requires electing the most efficient and effective scheme from as early as possible to allow for optimal assessment results (Congalton 2015). According to Congalton (2015), the scheme should include four components: *Definition*; Clearly defined rules for class definition; *Mutually exclusive*; No overlap can exist between classes; *Totally exhaustive*; The entire map must be included, and *Hierarchical*; More subclasses can exist to give further detailed options for assessment. Sources of error are equally as important as the requirement for the relationship between the sensed data and the reality on the ground to be as accurate as practicable, to mitigate any potential error and maintain a reliable outcome (Congalton 2015). It is also important that a sample size sympathetic to the research site is selected, with a recommendation of "…50 samples per thematic map class (maps less than about 500,000 ha and 12 or less thematic map classes)" (Congalton 2015, p. 593).

The assessment of the error matrix is straight forward, calculating and interpreting three separate accuracies. These consist of the user's accuracy, which specifies the quantity of a class on the map against the quantity of that class which exists on the ground. Producers accuracy indicates how often a class on the ground has been recorded as the same class on the digital map. Overall accuracy expresses the percent of classes that were accurately identified between reality and the resultant map (Congalton 2015) (*see Figure 2.4*).

Map \ Reference data	F	OV	D	W	Row total
F	55	11	4	3	73
OV	6	51	5	8	70
D	0	8	55	9	72
W	4	7	3	62	76
Column total	65	77	67	82	291

Land cover categories
F = Forest
OV = Other vegetation
D = Developed
W = Water

Overall accuracy = (55 + 51 + 55 + 62)/291 = 123/291 = 77%

Producer's accuracy
F = 55/65 = 85%
OV = 51/77 = 66%
D = 55/67 = 82%
W = 62/82 = 75%

User's accuracy
F = 55/73 = 75%
OV = 51/70 = 73%
D = 55/72 = 76%
W = 62/76 = 82%

***Figure 2.4** Error matrix showing the calculations for overall, producer's, and user's accuracies. (Congalton 2015).*

Having derived an error matrix, the technique called Kappa analysis provides the KHAT statistic which is an additional method to test the accuracy of a thematic map and its inherent classification success (Cohen 1960, cited in Congalton 2015 p. 597). According to Congalton (2015) the statistic is computed by indirectly incorporating the errors through the sums of row and column totals.

2.5 Image Classification

Image classification is the process of extracting information classes from a remote sensed image. It was initially developed in the 1980's and was based upon a pixel having a single cover class assigned to it. Since this time pixel-based methods have progressed along with subsequent techniques being developed, such as Object based Image Analysis (OBIA) and image segmentation, as well as Hybrid classification (Li et al. 2014).

2.5.1 Supervised Classification

The supervised classification technique involves three successive components: training, allocation and testing (Foody and Mathur 2004). Training is where a user defines a landcover type by selecting a region in an image to be representative of this and software is then able to recognise the spectral properties of that object. It is beneficial to select these areas from all over the scene to aid in accuracy due to the likelihood of natural differences between sites (Foody & Mathur 2004). Additionally, according to Mather and Piper (cited in Foody & Mathur 2004) to provide the best opportunity to calculate an accurate mean and variance and therefore an optimum result, it is important to have a minimum of "…10-30 independent training cases per class". The allocation process takes the established quantitative descriptions and training statistics and are used in conjunction with a training rule (such as maximum likelihood) and assigns each pixel to the class that it best represents (Blakey 2015; Foody & Mathur 2004). The testing process requires a separate assessment, in which Hammond and Verbyla (cited in Foody & Mathur 2004) recommend testing for the outcome of the classification process should be conducted using different image scenes to the training scenes, to avoid optimistic bias.

2.5.2 Pixel Based Classification

Pixel based classification is the original technique of analysing ground objects using the spectrometric processes on an individual pixel, with development beginning in the 1970s (Schowengerdt, 2007; Liang, 2004, cited in Veljanovski et al. 2011 p. 667). Pixel based classification according to Myint et al. (2015) and Kumar (2003), assigns pixels to classes by utilising both the spectral signal and ancillary information taken from that pixel resulting in numerical base to classify the pixels from. Further, different ground objects produce various combinations of digital numbers and therefore different spectral signals. Therefore, remote sensing and a per-pixel approach is understood to be an assembly of individual pixels containing individual spectral data which are used by classification systems such as supervised and unsupervised to allocate them to certain classes.

Scale suitability (i.e. pixel size) along with the spatial resolution of the sensor is important, by restricting the user with classification type, range, and accuracy of land cover, due to objects not being the same size as a pixel or of an appropriate shape (Myint et al. 2015).

2.6 Historical Monitoring of Seagrasses in the Gippsland Lakes

Research with a primary focus on seagrass in the Gippsland Lakes has been conducted in two separate studies. Roob and Ball's (1997) research was the first to focus on the spatial distribution and mapping of seagrass in the Gippsland Lakes. In 1997, they established that the most efficient method to map the seagrass locations was the use of remote sensing, utilising historical aerial photography images sourced from the Central Plan Office (CPO) of the Office of the Surveyor General (until 1989) and from QASCO Pty Ltd (1997 imagery) (Roob and Ball 1997). Initially, 12 sites were selected for assessment, with suitability determined from Rigby's 1984 report which researched the ecology of fish in seagrass habitats in the Gippsland Lakes (Roob and Ball 1997). Through aerial imagery and discussions with Natural Resource and Environmental staff and due to image quality, only five of these sites were determined suitable to use, with a time series established between 1959 and 1997.

The second was conducted by Warry and Hindell in 2011, who assessed cover using underwater video transects between September 2008 and April 2011. This study was conducted on a wide range of sites throughout the Lake system, which included the same sites used by Roob and Ball in 1997, which were used for a direct comparison of seagrass cover within the Gippsland Lakes. Prior to these studies, in 1977 Ducker et al. undertook the first survey to identify and record the aquatic vegetation in the Gippsland Lakes.

2.6.1 Site Descriptions

The selection of research sites is primarily based off Roob and Ball's research and provides a broad range of geographical locations within the Gippsland Lakes and therefore diversity of the conditions experienced at each. These include differing levels of terrestrial runoff, delivered from the four main rivers depositing into the lake system and higher concentrations of salinity the closer to the permanent entrance, located east of Reeve Channel.

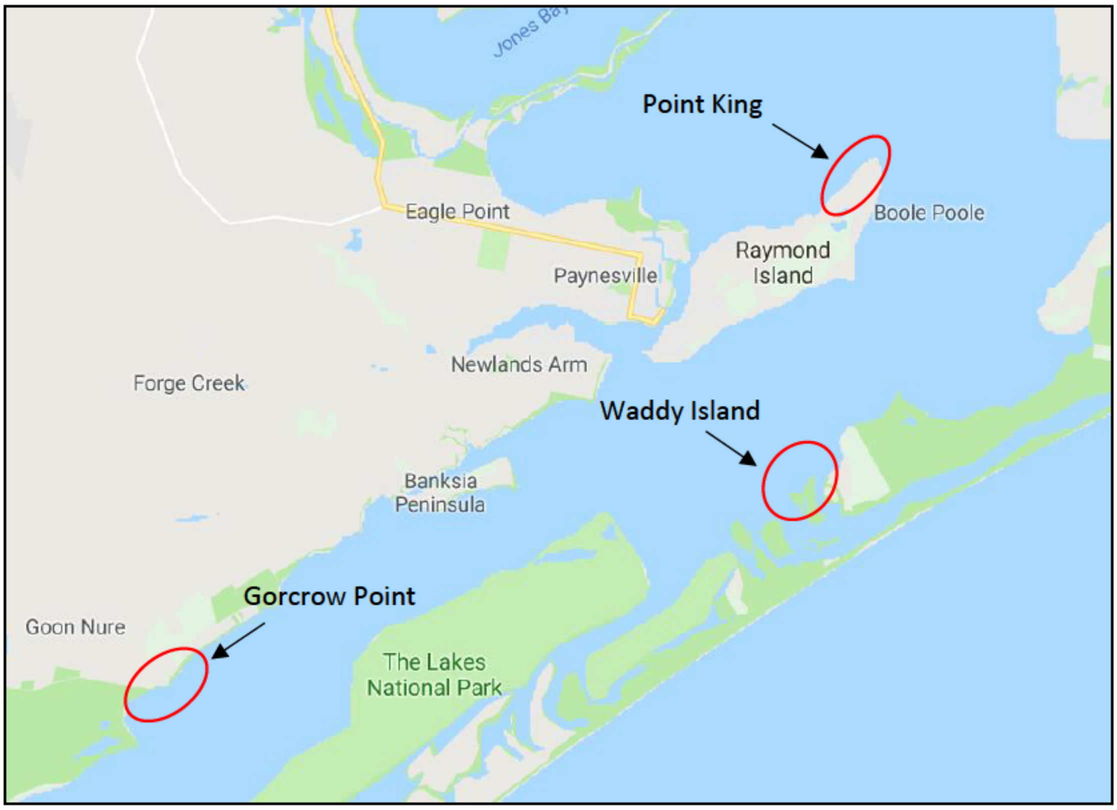

Figure 2.5 *An overview of the seagrass monitoring locations in the Gippsland Lakes (Google maps Australia 2019).*

Gorcrow Point - Steel Bay, Lake Victoria

Gorcrow Point is located in Lake Victoria and is the most western site in Roob and Balls study, along with the only south facing site. It is sheltered to the west by the larger Waddy Point and forms the eastern end of Steel Bay. Shallow sand banks follow the lake edge eastward along Steel Bay.

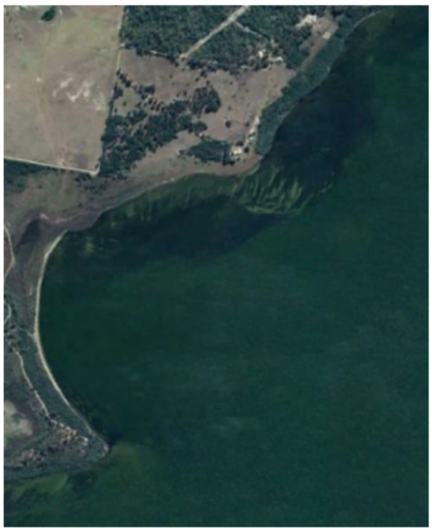

Figure 2.6 *Gorcrow Point – Steel Bay, Victoria project site (Google maps Australia 2019).*

Point King, Raymond Island, Lake King

Point King is the northern most tip of Raymond Island. It extends into Lake King and has substantial shallow sand banks to the north and west.

Figure 2.7 *Point King, Raymond Island in Lake King, Victoria project site (Google maps Australia 2019).*

Waddy Island, Lake Victoria

Waddy Island is located at the eastern end of Lake Victoria. This area features a series of deeper channels between neighbouring islands and shallow sand banks from the north east counter clockwise to the south west.

Figure 2.8 *Waddy Island, Victoria project site (Google maps Australia 2019)*

3.0 Research Methods

3.1 Introduction

This project is divided into two parts, the first being a comparison of three band (RGB) images and five band (RGB + NIR) to determine which is the most accurate. The second component of this project is the application of the proven combination to the projects pre-processed time series in order to monitor seagrass meadows. The work of Roob and Ball (1997) provides project sites to concentrate monitoring on and to help in correctly identifying seagrass meadows for supervised classification training areas. Additionally, Roob and Ball's 1997 and Warry and Hindell's 2011 results for seagrass cover, aid in determining possible trends in current research.

3.2 Landsat Data

3.2.1 Landsat Specifications

Where Landsat 7 and Landsat 5's operational times overlap (April 1999 – January 2013), Landsat 7 data will take precedence over Landsat 5 data. However, if optimal images cannot be obtained for the required dates, Landsat 5 data will be used to aid in the delivery of the best possible result.

Landsat 5

Landsat 5 was launched March 1st, 1984 and was equipped with Multispectral Scanner (MSS) and Thematic Mapper (TM) instruments. It had a 16 day repeat cycle and a 185 km swath which acquired imagery in the Worldwide Reference System-2 (WRS-2) path/row system (USGS n.d.). It continued to take EO's until it was decommissioned in January 2013.

Landsat7

Landsat 7 was launched April 15th, 1999 and was equipped with an Enhanced Thematic Mapper (ETM+) sensor. This is an improvement to Landsat 5's TM instruments and produces 8-bit imagery in 256 grey levels (USGS n.d.). Additionally, in May 2003 Landsat 7's Scan Line Corrector (SLC) failed. The SLC compensates for the forward motion of the satellite and without the SLC, the Landsat 7 sensor creates a zig-zag line of sight ground pattern which duplicates data (*Figure 3.1).* Within the initial processing, the duplication is removed, resulting in a loss of data as shown in *Figure 3.2*.

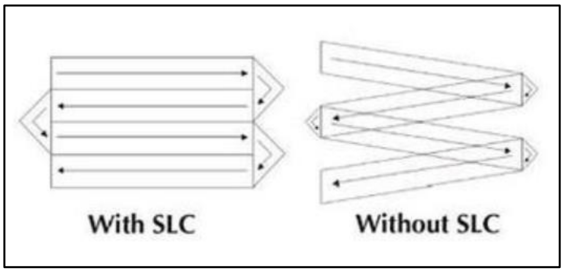

Figure 3.1 *Without SLC, the satellite now produces a zig-zag pattern along the ground track.*

Figure 3.2 *Diagonal data gaps run through Point King and Waddy Island study sites, in images between 2004 and 2017.*

Table 3.1 *Landsat series imaging instrument parameters. Of importance to this project are the TM (Landsat 5) and ETM+ (Landsat 7) columns (Eo portal n.d.).*

Landsat sensor	**MSS** (LS-1-5)	**TM** (LS-4/5)	**ETM** (LS-6)	**ETM+** (LS-7)
Spectral bands (all bands in µm)	1) 0.5 - 0.6 2) 0.6 - 0.7 3) 0.7 - 0.8 4) 0.8 - 1.1	1) 0.45 - 0.52 VNIR 2) 0.52 - 0.60 VNIR 3) 0.63 - 0.69 VNIR 4) 0.76 - 0.90 VNIR 5) 1.55 - 1.75 SWIR 7) 2.08 - 2.35 SWIR 6) 10.4 - 12.5 TIR	P) 0.52 - 0.90 VNIR 1) 0.45 - 0.52 VNIR 2) 0.52 - 0.60 VNIR 3) 0.63 - 0.69 VNIR 4) 0.76 - 0.90 VNIR 5) 1.55 - 1.75 SWIR 7) 2.08 - 2.35 SWIR 6) 10.4 - 12.5 TIR	P) 0.52 - 0.90 VNIR 1) 0.45 - 0.52 VNIR 2) 0.53 - 0.61 VNIR 3) 0.63 - 0.69 VNIR 4) 0.78 - 0.90 VNIR 5) 1.55 - 1.75 SWIR 7) 2.09 - 2.35 SWIR 6) 10.4 - 12.5 TIR
Swath width	185 km	185 km	185 km	185 km
Spatial resolution	80 m	30 m VNIR/SWIR 120 m TIR	15 m PAN, 30 m VNIR/SWIR, 120 TIR	15 m PAN 30 m VNIR/SWIR 60 m TIR
Radiometric resolution	6 bit	8 bit	9 bit (8 bit transmitted)	9 bit (8 bit transmitted)
Band-to-band registration		0.2 pixel (90%)	0.2 pixel (90%)	0.2 pixel (90%)
Geodetic accuracy without ground control		500 m (90%)	1000 m (90%)	400 m (90%)
Data rate	15 Mbit/s	85 Mbit/s	2 x 85 Mbit/s	2 x 75 Mbit/s
Instrument mass	64 kg	258 kg	288 kg scanner, plus 81 kg AEM	318 kg scanner, plus 103 kg AEM, plus 20 kg cable harness
Average power	50 W	332 W	490 W	590 W
Telescope aperture	23 cm	40.6 cm	40.6 cm	40.6 cm

The acquisition of data that is suitable for accurate processing and outcomes is a crucial component of this study and therefore, I have chosen to obtain data images in mid-summer. This is due to having a low rainfall monthly mean totals, a high mean number of clear days and a low mean number of cloudy days (BOM 2018). These climate statistics, along with seagrass growth through spring and summer due to more solar radiation and warmer water (Warry & Hindell 2011), make it the most optimal time to source data for. Without conditions that are free of these negative factors, the visibility of the benthic layer where the seagrass is located is compromised, making it difficult to determine the extent of the meadow (Dekker, Anstee & Brando 2003 & Ferguson, Korfmacher 1997).

Selecting bands within the visible spectrum (0.45-0.69) is required as spectral reflectance is restricted due to the radiated light having to penetrate the water column. More specifically band 1 (blue wavelength 0.45 - 0.52) in the Landsat 5 (TM) and Landsat 7 (ETM+) satellite spectral range is the most appropriate for bathymetric mapping (USGS 2018). This is due to water not being able to absorb the coastal aerosol band efficiently and therefore makes it appropriate for coastal water observation, and more specifically marine vegetation such as seagrasses (GIS Geography 2018 & Van Niel, Holmes & Radford 2009).

Table 3.2 *Optimal bands and wavelengths within the visible and near infrared ranges for the detection of both water and vegetation. (University of Southern Queensland 2018)*

Band number	Band name	Band width (μM)	Uses
1	Blue/Green	0.45–0.52	Designed for water body penetration, making it useful for coastal water mapping. Also useful for differentiation of soil from vegetation, and deciduous from coniferous flora.
2	Green	0.52–0.60	Designed to measure visible green reflectance peak of vegetation for vigor assessment.
3	Red	0.63–0.69	Very strong vegetation absorbence (Vegetation discrimination).
4	Near infrared	0.76–0.90	High land/water contrasts, very strong vegetation reflectance.

3.2.2 Surface Reflectance NBAR+ Data

Pre-processed Surface Reflectance NBAR+ data is obtained through Geoscience Australia's Surface Reflectance (SR) suite, with scenes being available for the entire Geoscience Australia archive (1987-present). This project focused on images from 1998 through to 2017, as this is where the time series analysis from Roob and Ball's (1997) previous research ended.

The images provide optical surface reflectance data for the Gippsland Lakes on path 91, row 86, within a 25m by 25m pixel. Corrections to image radiance values and the variations experienced due to atmospheric properties, and sun and sensor geometry have been applied to raw data to deliver a pre-processed product (Kool 2017).

3.3 Project Software

The software being utilised for this project will be Geographic Resources Analysis Support System GIS (GRASS GIS), an open source, free downloadable Geographic Information System (GIS) software. GRASS GIS was initially developed as a military tool for land management and environmental planning by the U.S Army Construction Engineering Research Laboratories. GRASS GIS has been significantly developed since its inception and is used by both private and research sectors due to its capabilities for geospatial data management and analysis, image processing, graphics and map production and spatial modelling (GRASS GIS 2015). In comparison to other well-known open source software such as Quantum Geographic Information System (QGIS) which has an emphasis in cartography and map making, Grass GIS' strength is in data processing and analysis.

To obtain statistical results regarding which method is superior, Grass GIS has plug-in source codes available to perform applications such as a kappa analysis (error matrix). The program utilises two maps, one validated map for each combination (three band and five band).

Additionally, QGIS was used for certain procedures that were not found possible within Grass GIS, such as splitting binary vector files and clipping raster data to obtain masks.

3.4 Image Classification

A supervised classification approach of traditional pixel-based classification was used to establish training areas which require a homogenous sample for them to work. The calibration of the classifier will be performed on two random years of Landsat 5 and Landsat 7 imagery, one for each band combination and a validation on a different year for each band combination will then be completed. The classification rule set will consist of simple presence/absent classes (Lyons et al. 2012), which is chosen since there is no known field data to allow for the determination of more cover level classes. Once this is completed an error matrix will be formed to determine where improvements can be made. This process will be undertaken for both band combinations to resolve which has statistical superiority and will be then used to map the occurrence of seagrasses at the study sites.

3.4.1 Pixel Based

In Grass GIS, the supervised method is a two-step process which uses the *g.gui.iclass* program, where the user outlines regions of interest by calculating spectral signatures for an image (Kratochvilova & Petras). This is followed by the *i.maxlik* program which is a maximum-likelihood discriminant analysis classifier, which assumes that every class for each band has normally distributed statistical values and are then assigned to the most probable class. This component is based on the regions selected in this project and uses the results from the spectral signatures file created by the *g.gui.iclass* program which include the region means and covariance matrices. This process determines which spectral classes the pixels will be assigned to in the classification process and outputs a raster image (Shapiro & Wen 2015).

3.5 Accuracy Assessment

Having completed classification procedures for both band combinations of Landsat scenes, an error matrix will be formed for each which provides users, producers and overall accuracy results. Additionally, a Kappa analysis will be utilised through Grass GIS software which has a plug-in function command *r.kappa* to assess the accuracy of the classified Landsat scenes, by crossing the classified map layer with respect to reference map layer.

Table 3.3 *The error matrix outcomes for comparison of reference data and predicted outcomes (Smith 2014).*

```
Error Matrix
Panel #1 of 1
               MAP1
     cat#   1   2   3   4   5
 M     1    168 5   0   1   0
 A     2    1   44  0   5   0
 P     3    0   16  271 1   12
 2     4    42  247 0   42  0
       5    0   0   15  0   30
Col Sum     211 312 286 49  42

cat#    Row Sum
R    1      168        5         0         1         0       174
e    2        1       44         0         5         0       398
c    3        0       16       271         1        12       922
l    4       42      247         0        42         0      1777
a    5        0        0        15         0        30      2677
     5948
```

The result of the computation provides values on the diagonal that reflect the number of accurately classified cells and the other figures are misclassifications of other classes. The sum of the Col Sum shows the total number of reference cells that Grass GIS believes to have classified correctly and when the sum of the diagonal is divided by the sum of the column, the result represents the observed correct percentage.

Table 3.4 *shows Percent Commission column (cells incorrectly placed into a class) and the Percent Omission column (cells not placed into that class correctly), along with the estimated kappa value (statistical measure of agreement between two different classifiers of the same data) where 1 would mean agreeance between the classifiers (Smith 2014).*

Cats	% Commission	% Ommission	Estimated Kappa
1	3.448276	20.379147	0.954957
2	12.000000	85.897436	0.816327
3	9.666667	5.244755	0.858306
4	87.311178	14.285714	0.076615
5	33.333333	28.571429	0.650350

Kappa	Kappa Variance
0.525067	0.000350

Further analysis is then required to see which classes have been misclassified by investigating the Percent Commission column (cells incorrectly placed into a class) and the Percent Omission column (cells not placed into that class correctly) in the tabulated results. This helps to identify which classes are providing the most erroneous results. The kappa coefficient shows the statistical amount of agreeance between two classifiers, where the value 1 would be total agreeance (Smith 2014). A total kappa value is then provided for the whole map, however, according to Smith (2014) the range of this value to determine a level of agreement has not been universally agreed-upon and one should consider all the components and results of the report when analysing classification results.

This will determine the project outcome of which band combination is best suited to identify seagrass meadows. This identified method will then be applied to the entire time series to monitor the spatial distribution of the meadows at the predetermined locations.

3.6 Time Series

The monitoring for this project will utilise time series data that consists of Geoscience Australia Landsat 5 and Landsat 7 imagery (*see Figure 3.3*). It will be acquired at largely equal bi-annual epochs, in the southern hemisphere summer and upon research for suitable tiles, it was discovered that the month of January provided consistent cloud free scenes. Initially it will focus on scenes from after the completion of Roob and Balls 1997 study and has therefore begun in 1998 through until 2017, with *Table 3.5* providing the dates utilised.

If time permits, imagery from 1987 through to 1996 at bi-annual epochs will be acquired to broaden the projects time series for a more comprehensive historical result regarding spatial trends and to make comparison with Roob and Balls 1997 aerial photographic study of the Gippsland Lakes.

***Table 3.5** provides the dates of pre-processed Landsat data*

Year	Date	Satellite
1998	10 January	Landsat 5
2000	8 January	Landsat 7
2002	29 January	Landsat 7
2004	19 January	Landsat 7
2006	24 January	Landsat 7
2008	14 January	Landsat 7
2010	3 January	Landsat 7
2012	25 January	Landsat 7
2013	12 February	Landsat 7
2015	1 January	Landsat 7
2017	6 January	Landsat 7

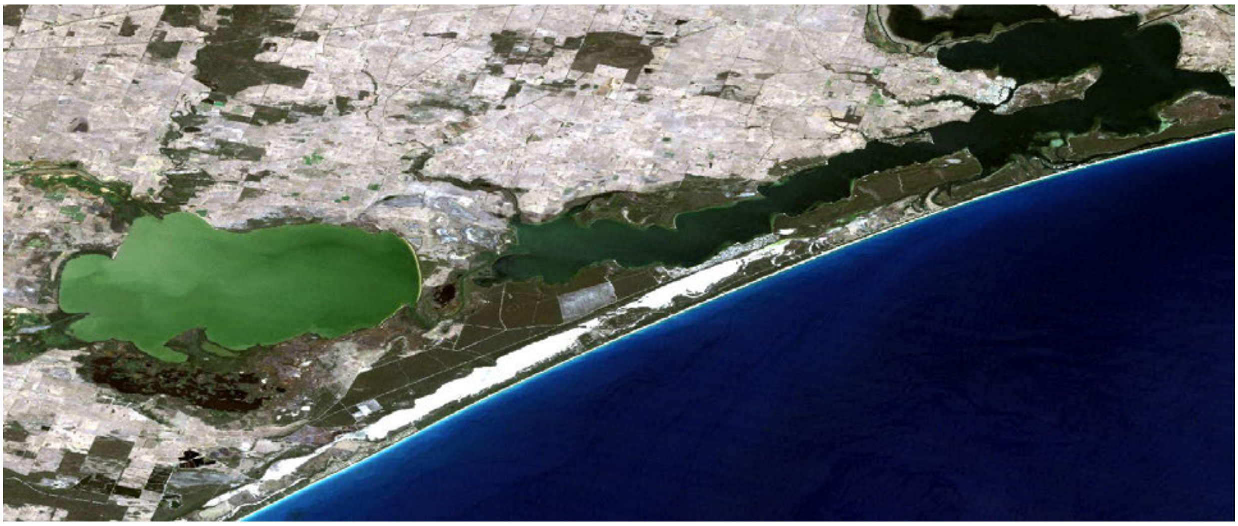

Figure 3.3 *Example of a pre-processed Landsat composite image utilised in the monitoring of seagrass in the Gippsland Lakes (10 January 1998). (Geoscience Australia 2019).*

3.7 Deep Water Mask

Being able to separate spectral properties and eliminate confusion of classes in the supervised classification process is critical in being able to achieve reliable identification results. As the shallow areas will consist of sand and seagrass, there will be a need to mask out the deep water, which can affect classification results. This is achieved through the calculation of a band ratio and utilising the spectral signatures of the desired classes to create a binary image, which consists of seagrass and sand areas (0) and deep water (1).

$$\frac{(Blue-Green)}{(Green-Red)} > x \tag{1.1}$$

Where x is the spectral signature ratio.

The resulting image is then vectorized, allowing for the classes to be split into two separate output files. Using the seagrass and sand file, a composite raster image can be clipped to output a final composite image of the required area to be classified.

4.0 Results and Discussion

4.1 Introduction

The methods described in this dissertation have been effectively applied to a time series of pre-processed Landsat 5 and Landsat 7 imagery. These techniques have produced realistic seagrass cover plots for each study site, which can be viewed in the following sections. The results indicate that the cost-effective methods produced in this project could be used for mapping seagrass cover in shallow waters of Australian coastal lake systems, without the need for extensive field surveys prior to monitoring.

It must be noted that discrepancies between the 1998-2002 epochs and 2004-2017 epochs can be seen, due to Landsat 7's Scan Line Corrector (SLC) failure in May 2003. The SLC compensates for the forward motion of the satellite. Without the SLC, the Landsat 7 sensor creates a zig-zag line of sight ground pattern which duplicates data (*Figure 3.1)*. Within the initial processing, the duplication is removed, resulting in a loss of data as shown in *Figure 3.2*. This loss of data affects each of the three study sites from 2004 onwards. Additionally, these diagonal lines of data loss change at each study epoch and can involve one stripe per site on one image and two stripes the following, which can skew pixel results due to the quantity and location of striping. This loss of data affects the ability to map class cover as the quantities are unknown under these areas, along with the pixel quantities derived from the image histograms, resulting in uneven study areas (study site pixel quantity). The 2013 epoch, across all three sites produced a result different to all other results after 2004. There was no loss of data shown (striping) and at both Point King and Waddy Island, there were long straight edges of seagrass cover, which appear to be an unnatural edge to a seagrass meadow. These discrepancies and abnormalities in output have made them unreliable and have therefore been excluded from the results and subsequent sections.

4.2 Supervised Classification Validation and Comparison

4.2.1 Three Band Comparison

Figure 4.3 *1998 Three Band (RGB) supervised classification*

Figure 4.4 *2010 Three Band (RGB) supervised classification*

Table 4.1 *provides the Grass GIS kappa analysis and error matrix for the 1998 and 2010, Three Band supervised classifications.*

Three Band Error Matrix 1998 & 2010			
Category	**Seagrass**	**Sand**	**Row Sum**
Seagrass	2069	590	2659
Sand	487	697	1184
Column Sum	2556	1287	3843
Category	**Commission %**	**Omission %**	**Estimated Kappa**
Seagrass	22.188793	19.053208	0.337440
Sand	41.131757	45.843046	0.381575
Kappa		**Kappa Variance**	
0.358153		0.000256	
Users Accuracy %		**Producers Accuracy %**	
Seagrass	78	**Seagrass**	81
Sand	59	**Sand**	54

Observations Correct	Total Observations	% Observed Correct
2766	3843	72

The supervised classification of Three band (RGB) images for 1998 and 2010 were used to validate the process through a Grass GIS kappa analysis. Of the 2556 seagrass pixels, 2069 were classified correctly, with the remaining 487 being misclassified as sand. Of the sand pixels, 697 were classified correctly and 590 misclassified as seagrass. The correctly classified classes are then used to compute the overall accuracy of 72%.

Seagrass users, producers and total accuracies are reported at 78%, 81% and 72% respectively.

4.2.2 Five Band Comparison

Figure 4.5 *1998 Five Band (RGB + NIR) supervised classification*

Figure 4.6 *2010 Five Band (RGB + NIR) supervised classification*

***Table 4.2** provides the Grass GIS kappa analysis and error matrix for the 1998 and 2010, Five Band supervised classifications.*

Five Band Error Matrix 1998 & 2010			
Category	**Seagrass**	**Sand**	**Row Sum**
Seagrass	2408	544	2952
Sand	405	586	991
Column Sum	2813	1130	3943
Category	**Commission %**	**Omission %**	**Estimated Kappa**
Seagrass	18.428184	14.397440	0.356971
Sand	40.867810	48.141593	0.427153
Kappa		**Kappa Variance**	
0.388921		0.000269	
Users Accuracy %		**Producers Accuracy %**	
Seagrass	82	**Seagrass**	86
Sand	59	**Sand**	52

Observations Correct	**Total Observations**	**% Observed Correct**
2994	3943	76

Of the 2813 seagrass pixels, 2408 were classified correctly, with the remaining 405 being misclassified as sand. Of the sand pixels, 586 were classified correctly and 544 misclassified as seagrass. The correctly classified classes are then used to compute the overall accuracy of 76%.

Seagrass users, producers and total accuracies are reported at 82%, 86% and 76% respectively.

4.3 Time Series Results

4.3.1 Gorcrow Point

Gorcrow Point had an unstable period between 1998 and 2008 seeing significant fluctuations in seagrass cover. Within this period, 2000, 2004 and 2008 the seagrass cover was considerably less than sand, with 2004 having the least amount of cover (133 pixels). In 2002 and 2006 the seagrass cover was considerably more than sand with maximums of 483 and 531 respectively.

From 2010 to 2017, the seagrass cover shows an upward trend of spread, with more seagrass than sand at each epoch. This period finishes with the maximum level of cover for the research period (544 pixels) and second lowest value for sand (47 pixels). The cover does not report to follow a pattern, however the central area of the site on the point is the last area to receive seagrass growth, with 2006 being the only period of cover. Seagrass has a consistence presence in the south western section of the site.

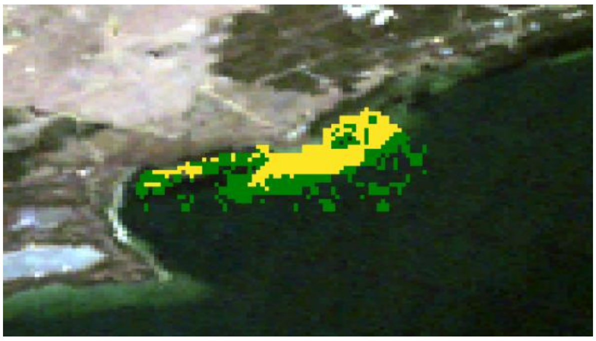

Figure 4.7 *Gorcrow Point 10 January 1998*

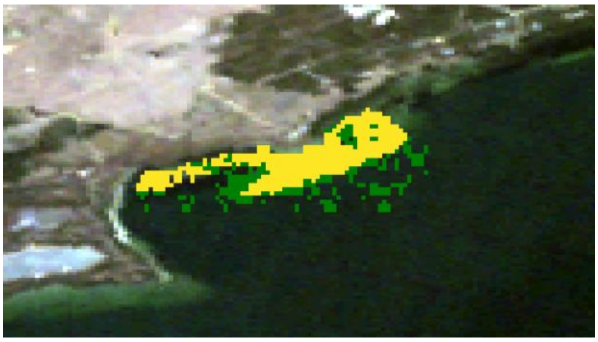

Figure 4.8 *Gorcrow Point 8 January 2000*

Figure 4.9 *Gorcrow Point 29 January 2002*

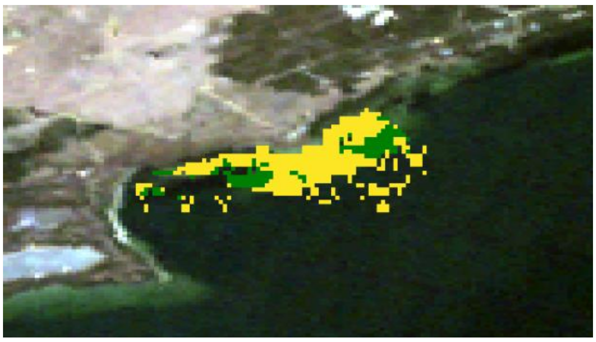

Figure 4.10 *Gorcrow Point 19 January 2004*

Figure 4.11 *Gorcrow Point 24 January 2006*

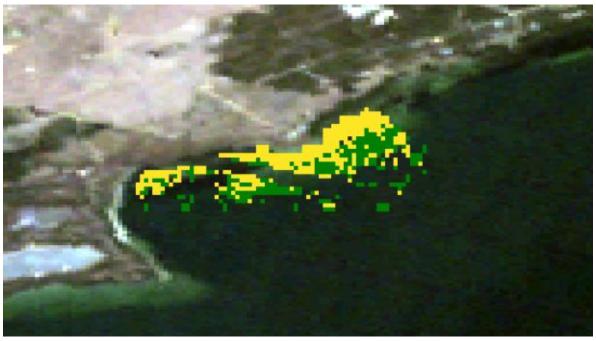

Figure 4.12 *Gorcrow Point 14 January 2008*

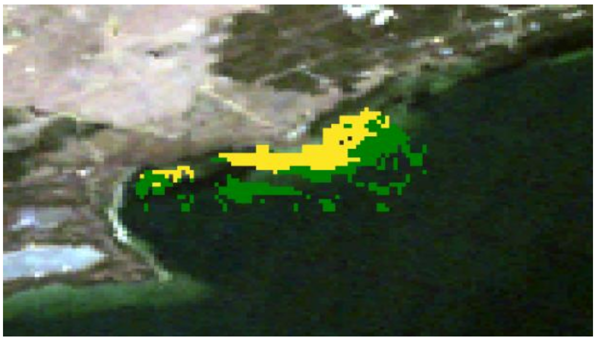

Figure 4.13 *Gorcrow Point 3 January 2010*

Figure 4.14 *Gorcrow Point 25 January 2012*

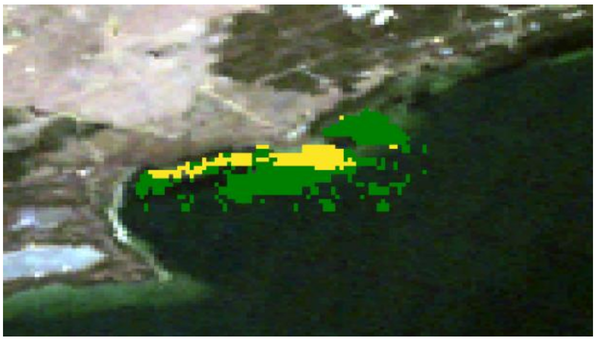

Figure 4.15 *Gorcrow Point 1 January 2015*

Figure 4.16 *Gorcrow Point 6 January 2017*

Table 4.3 *Shows pixel class quantities and the resulting sum. The pixel standard sums for each project site changes to inconsistent values between 2002 and 2004, coinciding with the SLC failure.*

Gorcrow Point	**Band**		
Year	**Seagrass (1)**	**Sand (2)**	**Sum**
1998	361	276	637
2000	233	404	637
2002	483	154	637
2004	133	438	571
2006	531	4	535
2008	237	306	543
2010	315	230	545
2012	306	279	585
2015	441	141	582
2017	544	47	591

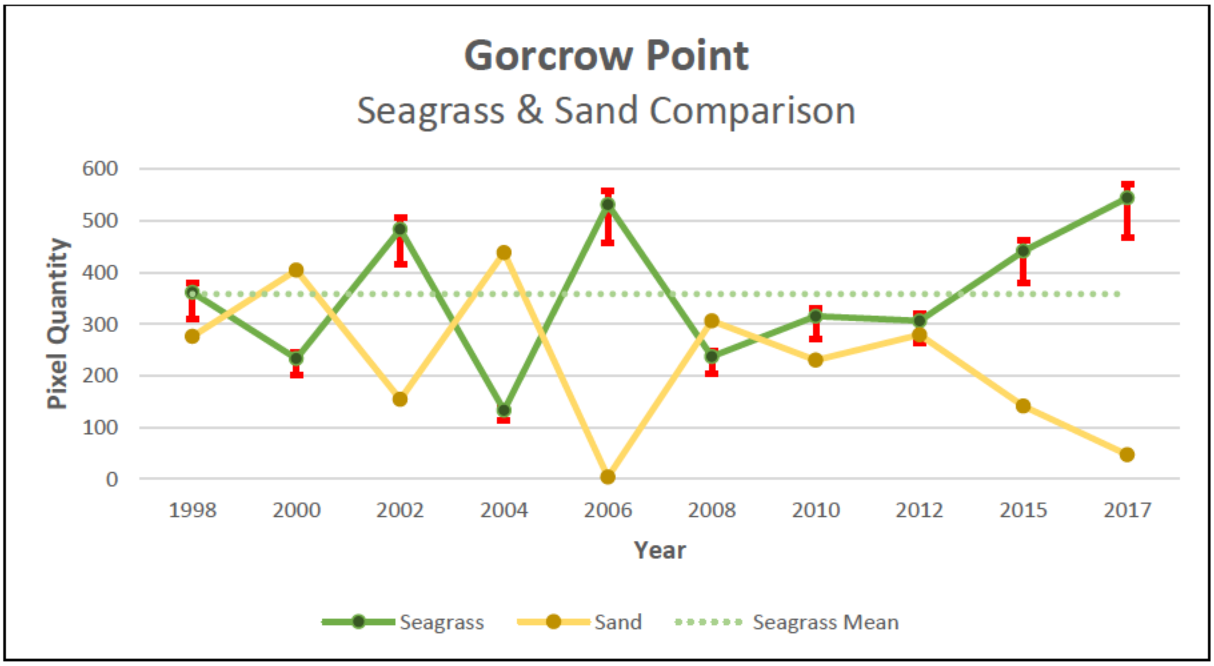

Figure 4.17 *Gorcrow Point Seagrass and Sand pixel quantity comparison. The variability and uncertainty of data is represented by error bars for seagrass cover, which is calculated from user and producer accuracy results.*

4.3.2 Point King

Point Kings seagrass cover shows a gradual, general decline over the entire time series. It is at its highest levels in the first two epochs in 1998 and 2000, with a maximum of 591 pixels recorded in 2000. The last five epochs are the lowest in the time series with a minimum of 92 pixels in 2012. The growth and die-off of seagrass at this site does not follow a common pattern, with only the south west end of the site reporting to have a consistent patch of seagrass.

2006 is of interest, having the lowest pixel count which is attributed to having two lines of no data due to SLC failure. Additionally, 2006 has a 100% cover of seagrass, which is unlikely however, the two years either side show sand present in the regions of missing data.

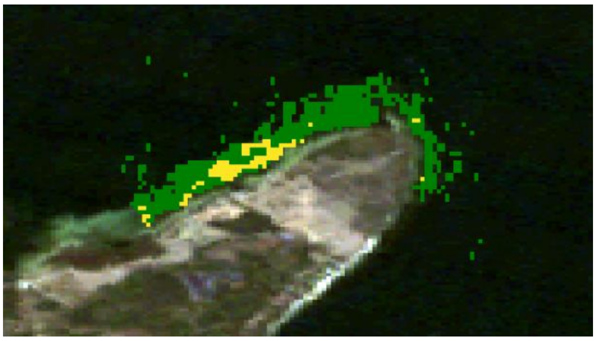

Figure 4.18 *Point King 10 January 1998*

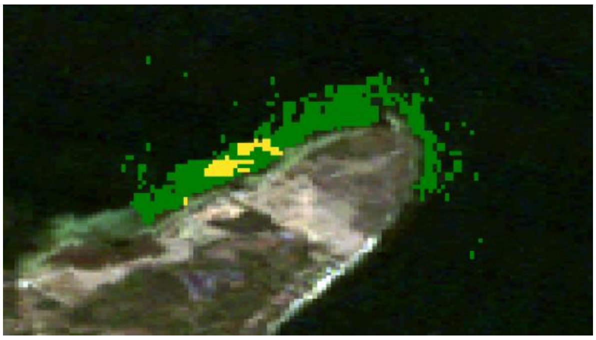

Figure 4.19 *Point King 8 January 2000*

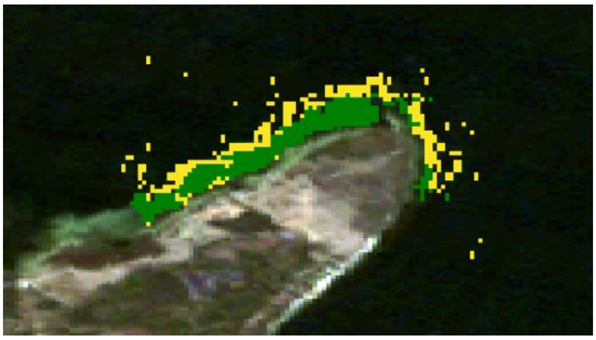

Figure 4.20 *Point King 29 January 2002*

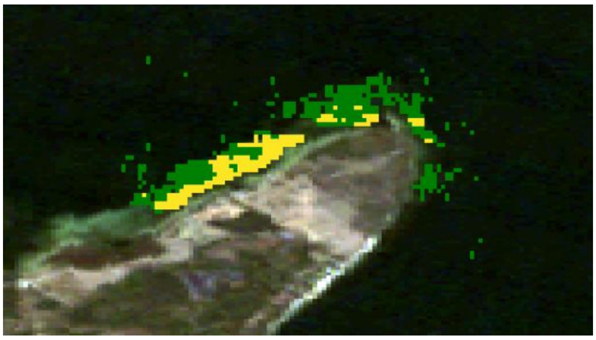

Figure 4.21 *Point King 19 January 2004*

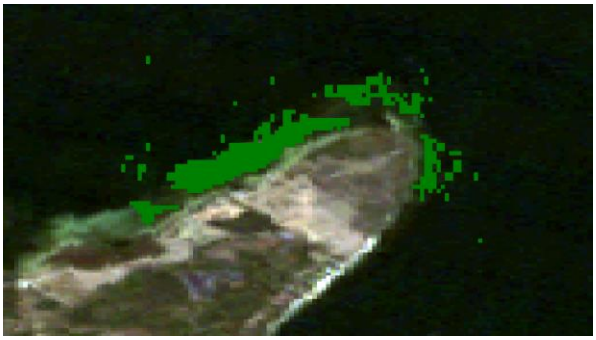

Figure 4.22 *Point King 24 January 2006*

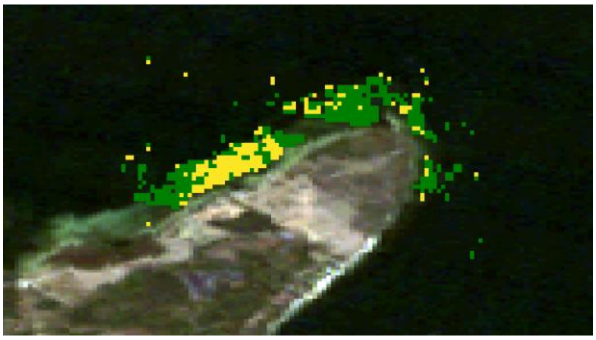

Figure 4.23 *Point King 14 January 2008*

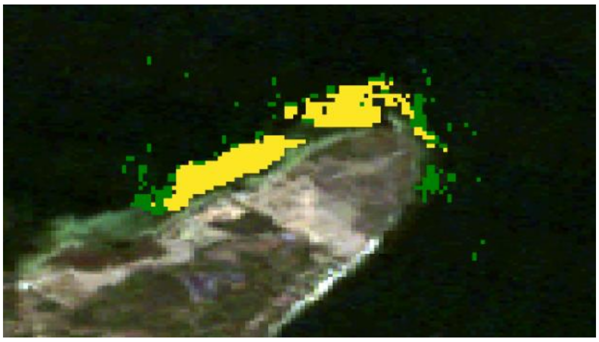

Figure 4.24 *Point King 3 January 2010*

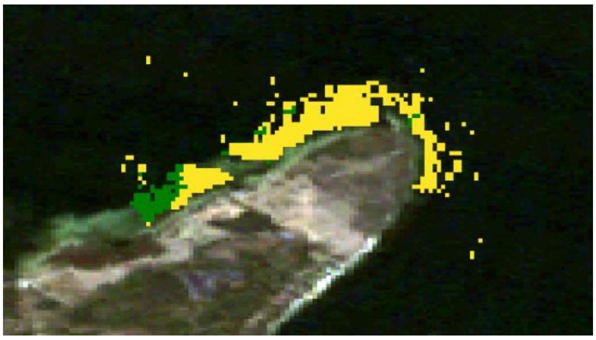

Figure 4.25 *Point King 25 January 2012*

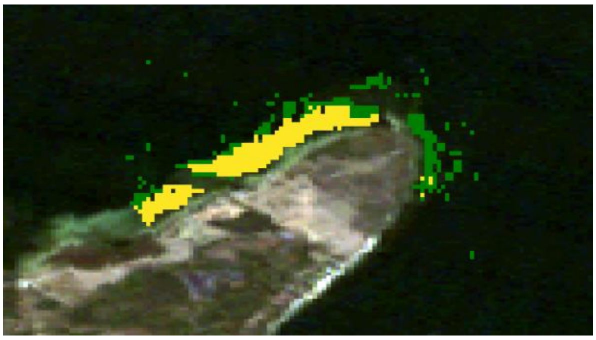

Figure 4.26 *Point King 1 January 2015*

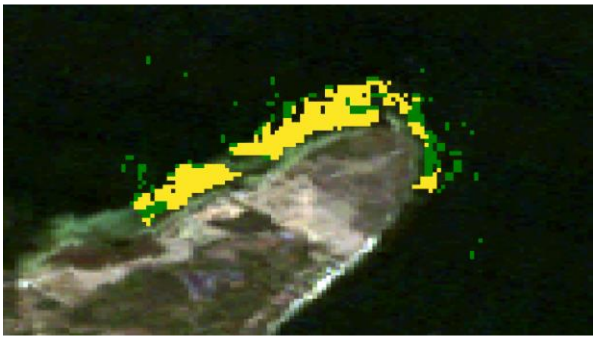

Figure 4.27 *Point King 6 January 2017*

Table 4.4 *Shows pixel class quantities and the resulting sum. It can be seen that the pixel standard sums for each project site changes to inconsistent values between 2002 and 2004, coinciding with the SLC failure.*

Point King	Band		
Year	**Seagrass (1)**	**Sand (2)**	**Sum**
1998	565	88	653
2000	591	62	653
2002	364	289	653
2004	393	179	572
2006	489	0	489
2008	379	174	553
2010	178	394	572
2012	92	491	583
2015	237	295	532
2017	174	417	591

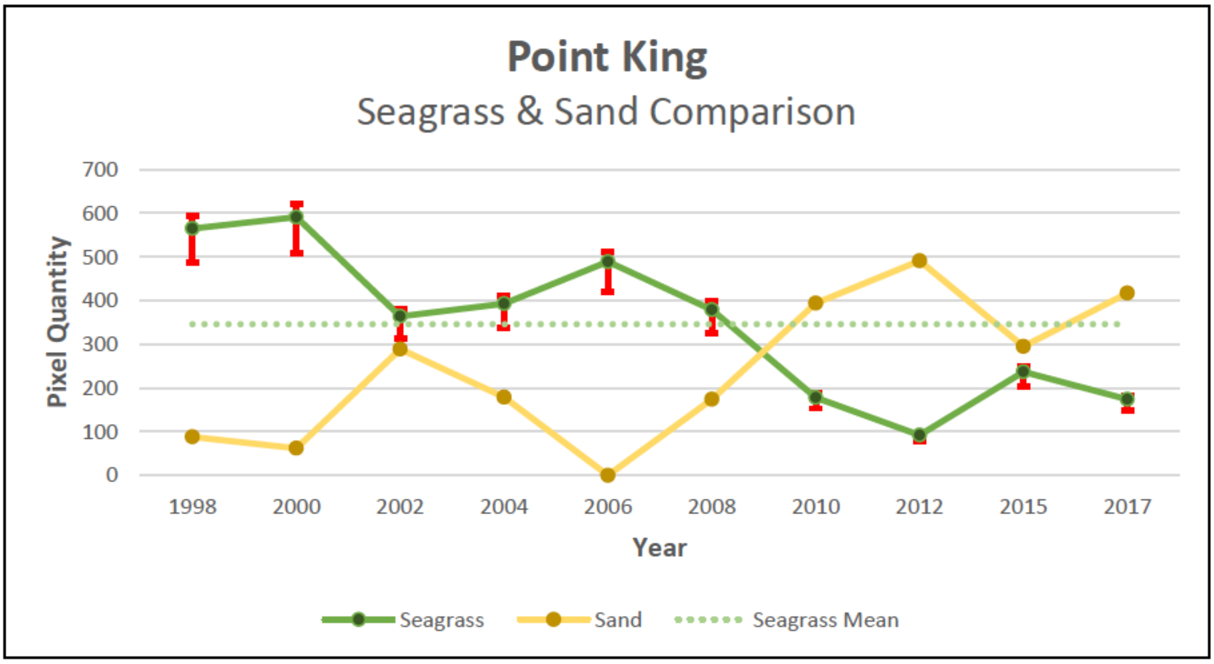

Figure 4.28 *Point King Seagrass and Sand quantity comparison. The variability and uncertainty of data is represented by error bars for seagrass cover, which is calculated from user and producer accuracy results.*

4.3.3 Waddy Island

Waddy Island proved to be the most consistent of the three study sites (70% above average cover), having only two epochs of greater sand coverage, albeit marginally. Either side of the period 2004 to 2008, very good cover exists for the rest of the time series. The maximum cover was experienced in 2002, recording 2210 pixels and a minimum cover level of 1022 pixels in 2006. The trend of change between seagrass and sand is generally consistent through the time series, with a central sand bank that is never completely covered by seagrass. The remainder of this site experiences differing patterns, with the western end of the site predominantly being an area with generally consistent seagrass cover.

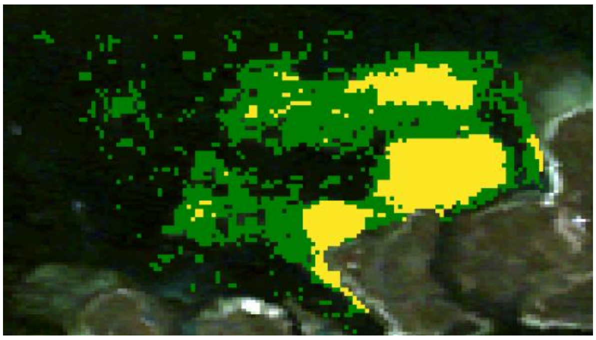

Figure 4.29 *Waddy Island 10 January 1998*

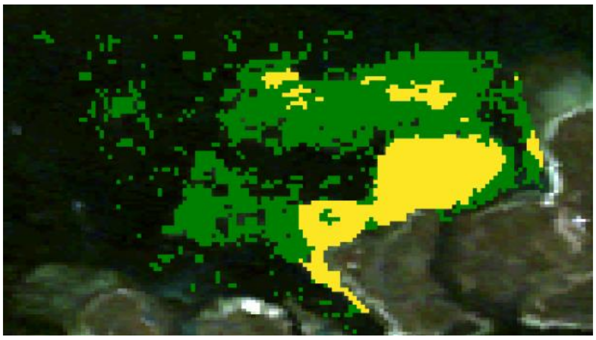

Figure 4.30 *Waddy Island 8 January 2000*

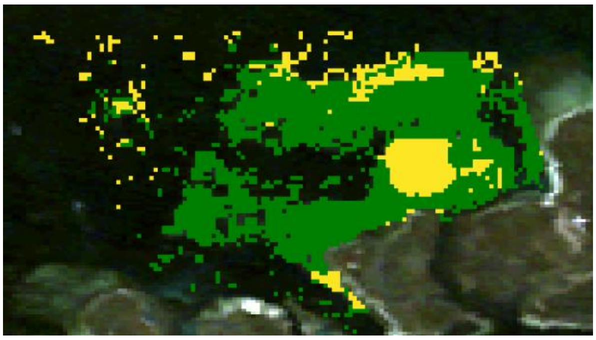

Figure 4.31 *Waddy Island 29 January 2002*

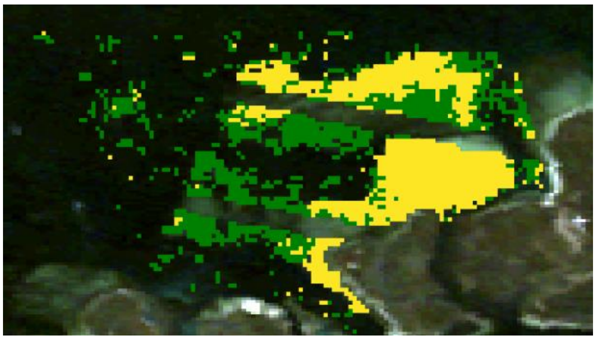

Figure 4.32 *Waddy Island 19 January 2004*

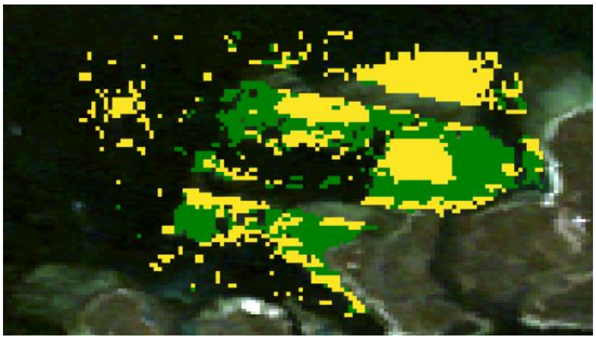

Figure 4.33 *Waddy Island 24 January 2006*

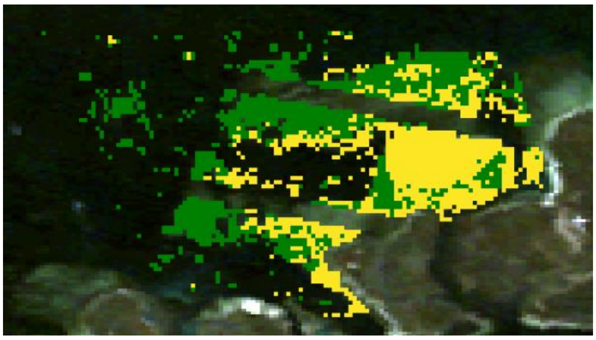

Figure 4.34 *Waddy Island 14 January 2008*

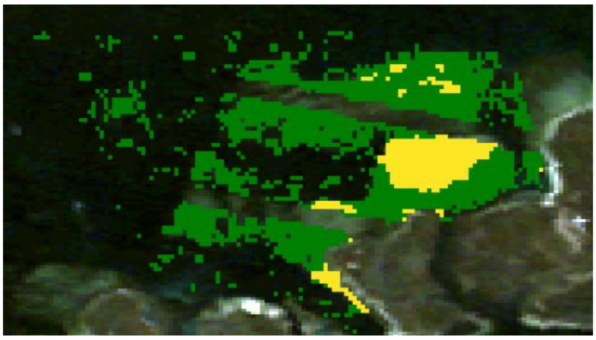

Figure 4.35 *Waddy Island 3 January 2010*

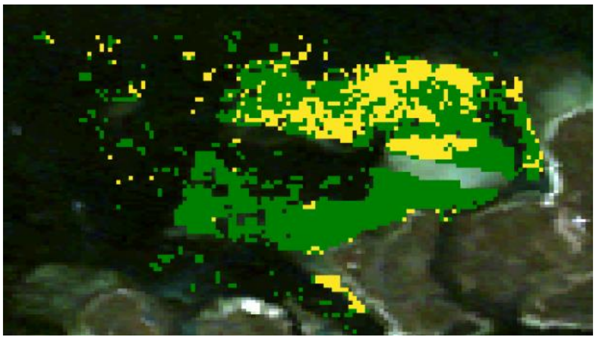

Figure 4.36 *Waddy Island 25 January 2012*

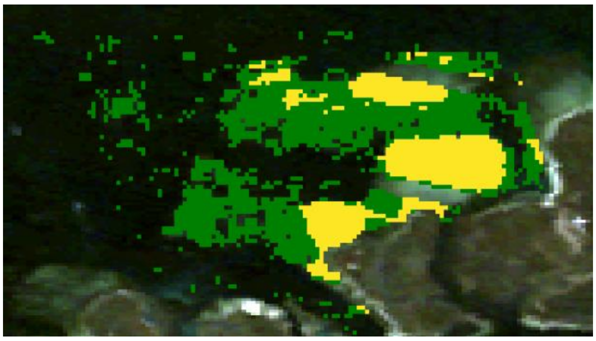

Figure 4.37 *Waddy Island 1 January 2015*

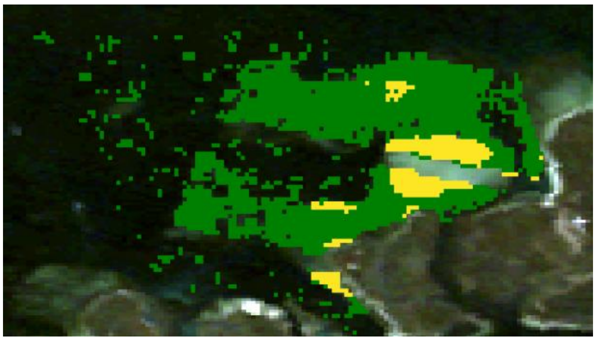

Figure 4.38 *Waddy Island 6 January 201*

Table 4.5 *Shows pixel class quantities and the resulting sum. The pixel standard sums for each project site changes to inconsistent values between 2002 and 2004, coinciding with the SLC failure.*

Waddy Island	Band		
Year	**Seagrass (1)**	**Sand (2)**	**Sum**
1998	1849	892	2741
2000	1915	826	2741
2002	2210	531	2741
2004	1113	1115	2228
2006	1022	1221	2243
2008	1184	1043	2227
2010	1876	367	2243
2012	1709	630	2339
2015	1688	742	2430
2017	2063	289	2352

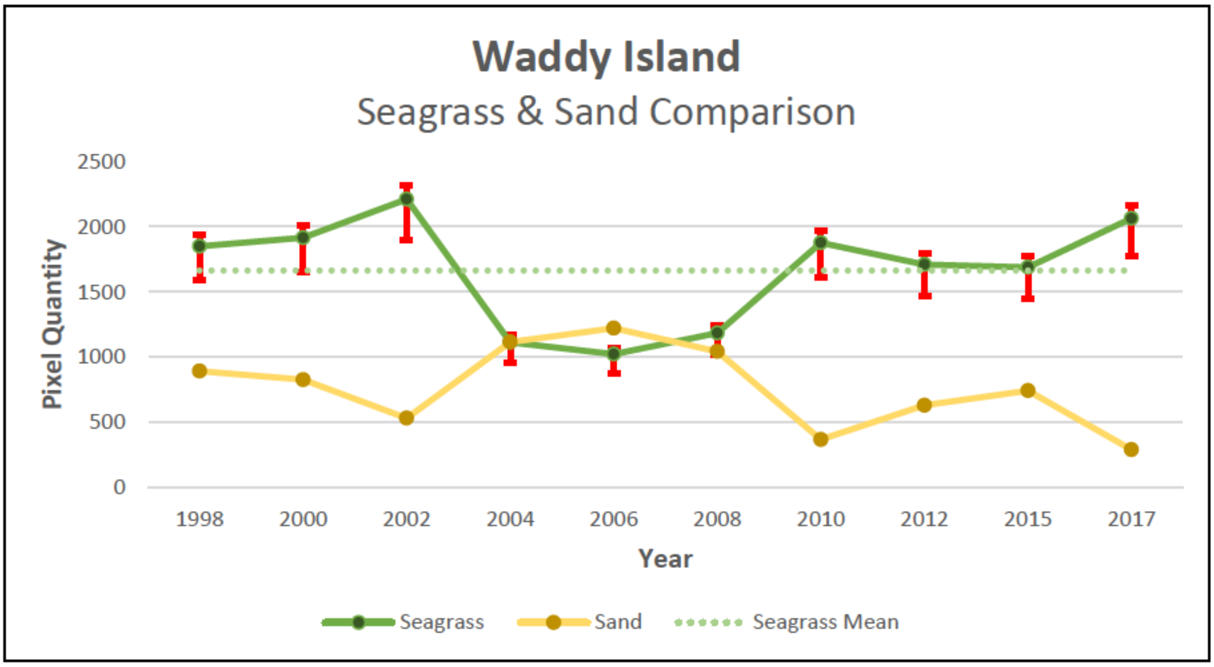

Figure 4.39 *Waddy Island Seagrass and Sand quantity comparison. The variability and uncertainty of data is represented by error bars for seagrass cover, which is calculated from user and producer accuracy results.*

4.3.4 Project Site Comparison

All sites through the time series period displayed dissimilar results. This is evident with a minimum of one result disagreeing with the other sites at each bi-annual epoch. When converted to a percentage level, the results can exaggerate the actual results, such as at Point King, which saw a general decline overall, however in *Figure 4.40*, the year 2006 shows a spike to 100% which when compared to the comparison results in *Figure 4.28* and the surrounding epochs, this actually gives a false indication of seagrass cover. However, when the other epochs are viewed away from these exaggerations, there is a general shared trend upward at Gorcrow Point and Waddy Island from 2008 until 2017 and can be seen along with a disagreement in condition direction, as Point King decreases through the same period.

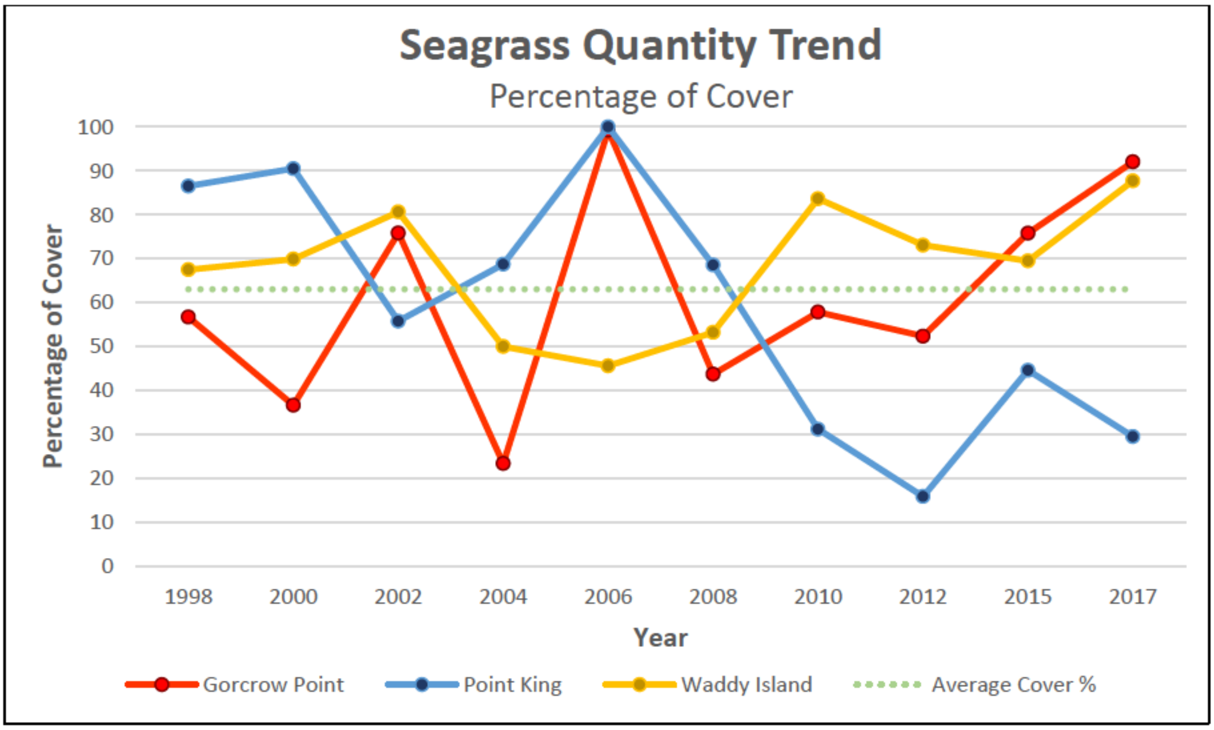

Figure 4.40 *Seagrass quantity trend of Gorcrow Point, Point King and Waddy Island converted to a percentage to allow for ease of comparison.*

4.4 Discussion

The aim of this research was to establish a cost-effective and reliable method for ascertaining the spatial distribution of seagrass meadows in the Gippsland Lakes, using remote sensed satellite imagery between 1998 and 2017. The results indicate a correlation between past research and this study, with each study site displaying similar general trends and change in cover at key dates which are linked to local environmental events. However, when investigating a single image date, the three study sites displayed varying results. This showed that results are site specific and are dependent on local conditions and a single site cover analysis cannot be used to identify the broad spatial condition of seagrass cover within the lake system. The reliability of this result was enhanced through testing of band combinations and strengthened through the validation of classifications using an error matrix with total accuracies of 76% achieved.

4.4.1 Gorcrow Point

As this study's time series begins the year following Roob and Ball's 1997 research, the 1998 epoch reported an average level of cover (*Figure 4.17*). This level of cover is above that stated by Roob and Ball who describe a sparse coverage, which is however the only result to show a discrepancy between this study and Roob and Ball's work.

Results at Gorcrow Point produced a similar trend between 1998 and 2008, to what was discovered in Roob and Ball's 1997 research between three consecutive images in 1976, 1979 and 1984. In both these periods, seagrass cover would increase before experiencing a period of die-back and then another period of growth. This pattern was more sustained in this project, as there were more measurement epochs in the study. From 2008 an upward trend was apparent through to 2017, where the highest cover of seagrass was recorded. Warry and Hindell's (2011 p.20) report for the Gorcrow Point site can not be directly compared due to their site's location being only to the east of Gorcrow Point. However, a broad correlation exists in the spatial trend with Warry and Hindell's (2011) results in the 2009 and 2011 research epochs, exhibiting levels of 50% or greater cover, which is labelled as a mid-level (3/5) cover condition and compares with this studies results. The decrease seen in 2010 in this same research however does not match with this studies results, as the levels remain generally consistent through this period and could be attributed to the marginally different geographical area.

4.4.2 Point King

Point King Study site has shown a general and gradual decline over the entire time series. The seagrass cover in the first two epochs of 1998 and 2000 shows the highest levels of cover recorded at this site, which agrees with Roob and Ball (1997), that found the highest seagrass cover level for that site in 1997. This agreement between the studies provides confirmation of accuracy at the start of the time series, between two different research methods.

The gradual trend of receding seagrass cover at point King is supported through the period of 2008 to 2011 in Warry and Hindell's (2011) research. It is reported that since Roob and Ball's 1997 report, that there is a decrease in seagrass density at the Point King site.

A decline in cover quantity could be attributed to environmental factors through the Point King study sites geographical proximity to three major rivers; Mitchell, Nicholson and Tambo (*Figure 4.41*), with outflows all being into Lake King. There are agricultural practices upstream in all three rivers with significant vegetable farming practices surrounding the Mitchell River near the lake system (EPA Victoria 2002). This could cause an increase in turbidity, thus reducing light and reducing growth along with a decrease in water quality with higher levels of agricultural runoff entering the water.

Figure 4.41 *Point King study site's geographical location in relation to the Mitchell, Nicholson and Tambo Rivers.*

4.4.3 Waddy Island

Waddy Island's results were the most consistent of the three sites, displaying high levels of seagrass cover for seven of the ten measurement epochs. The first result epoch in 1998 correlated with Roob and Ball's (1997) 1997 result, where they reported the highest level of cover that the Waddy Island study site had produced. This agreement between the findings provides confirmation of accuracy at the start of the time series, between two different research methods. Additionally, the overall trend of results at this site, being a trough with high levels of cover either side, follows that of Roob and Ball's (1997) results, with two successive years of increase, followed by a decrease and then two successive years of increase in cover.

However, there is a discrepancy in results with Warry and Hindell (2011) between April 2009 to 2010, where it was reported that there was a decline in seagrass condition due to an increase in epiphytic algal cover in the surrounding areas of Waddy Island. This however contrasts with what was seen in this projects results, with an increase in seagrass cover recorded at this time. This difference could be due to an erroneous result such as the supervised classification interpreting this epiphytic algal cover as seagrass, however, due to this project's aim and methodology of developing a cost-effective solution of not having to collect and use in-situ data, the difference was not investigated.

The results at Waddy Island differ to Gorcrow Point and Point King and could be attributed to local conditions, such as water quality and differing levels of salinity. This spatial trend is supported through Roob and Ball's (1997) research where it is noted that the pattern of change at the Waddy Island study site was generally different to that of other study sites.

4.4.4 Site Comparison

The ability to draw a conclusive and consistent trend that all three study sites exhibit would be beneficial in the ongoing sustainable management of such a crucial ecosystem. However, the results obtained show wide variances at each site, with at least one result disagreeing with other results at each bi-annual epoch. This variation was also identified by Roob and Ball (1997), where it was reported that the data indicates that trends are not consistent throughout the Gippsland Lakes. This inconsistency between study sites leads the study to conclude that each result is site specific and are dependent on local conditions and a single site result is not enough in determining the whole of seagrass conditions within the Gippsland Lakes.

4.4.5 Limitations

This study has some limitations. Through the use of Landsat data, which is by design a medium resolution product and outputs a spatial resolution of 25 meters. The spatial bounds of seagrass meadows, however, do not spread naturally to meet such extents. Therefore, limitations are present with recording the actual extents of a seagrass meadows edge and thus, there will be some pixels that are classified as seagrass that also contain sand and others that are classified as sand that contain areas of seagrass. This study did not intend to look at this factor and therefore has not investigated nor allowed for this factor in the methodology or results. This constraint can be mitigated by using high spatial resolution satellite imagery, such as World view 2. This satellite has a spatial resolution of 1.84 m (Satellite Imaging Corporation n.d.), which would significantly enhance the ability to precisely map seagrass cover extent.

Additionally, it was beyond the scope of this study to use a greater concentration of scenes in the time series, however, this could expand the understanding of seagrass patterns and quality of data collected by Landsat. This could be achieved through the utilisation of a denser time series, which could be employed at a sub annual level, to allow for greater interpretation of results. Using data from different seasons would provide a more detailed pattern of natural seagrass cycles, along with providing different physical conditions in which the satellites sense and collect data.

However, having discussed these limitations, they do not impact on the ability of the project to deliver a reliable outcome, with Landsat data being successfully used to report spatial seagrass cover in several studies such as Lyons et al. (2010), Roelfsema et al. (2009) and Dekker et al. (2003), along with time series' that are of lesser length and or of a wider epoch date range.

5.0 Conclusion

Through the use of pre-processed Landsat satellite data, this research aimed to produce a cost-effective and reliable method to monitor seagrass cover in the Gippsland Lakes, Victoria, Australia. A successful outcome negates the need for the expensive collection of in-situ field data and provides insight into the spatial patterns of local seagrass meadows.

The use of remote sensed data was used as it is freely available and allows for the construction of a detailed, historical time series to produce temporal maps, which can aid in the sustainable management of vital ecosystems such as seagrass meadows. The results this project sought, were to obtain reliable seagrass cover estimates and patterns, that extended and agreed with past research results at corresponding study sites. This was done using free of charge pre-processed Landsat 5 and Landsat 7 data obtained through Geoscience Australia, which were processed with open sourced software, Grass GIS and QGIS. This process generated results that provided a two-class seagrass and sand thematic map with a total accuracy of 76% achieved. All three study sites displayed general values and trends that correlated with previous research, which shows a positive outcome to the project aim and the ability to map seagrass cover without in-situ data.

5.1 Further work

To enhance the aim and outcomes that this project implemented, there are some opportunities for further work.

- Using a greater concentration of scenes within a year so that more detailed trends could be identified.
- Use high spatial resolution satellite imagery, such as World view 2 to provide a more accurate map of the spatial extents of seagrass meadows.
- Select a greater number of study sites, to develop a more complex understanding of the whole of the Gippsland Lakes’ seagrass cover.
- Research differences in spectral signatures between seagrass, algae and other macro aquatic species in order to separate classes and obtain more accurate results.
- Explore different classification techniques such as object-based image analysis, to increase mapping detail and accuracy.

6.0 References

Al-doski, J Mansor, S & Shafri, H 2013, 'Image Classification in Remote Sensing', *Journal of Environment and Earth Science*, vol. 3, no. 10, viewed 11 May 2019, <https://pdfs.semanticscholar.org/f5ed/fbb09d8f12c59017753f67160aa0c5af6588.pdf>.

Al-doski, J Mansor, S and Shafri, H 2013, 'Image Classification in Remote Sensing', *Journal of Environment and Earth Science*, vol. 3, no. 10, viewed 23 April 2019, <https://pdfs.semanticscholar.org/f5ed/fbb09d8f12c59017753f67160aa0c5af6588.pdf>.

Bhosale, N Manza, R and Kale, K 2014, 'Analysis of Effect of Gaussian, Salt and Pepper Noise Removal from Noisy Remote Sensing Images', *Proceedings of the Second International Conference on "Emerging Research in Computing, Information, Communication and Applications"*, viewed 14 May 2019, <https://www.researchgate.net/publication/304322211_Analysis_of_Effect_of_Gaussian_Salt_and_Pepper_Noise_Removal_from_Noisy_Remote_Sensing_Images>.

Blake, S Roob, R & Patterson, E 2000, *Seagrass Mapping of Victoria's Minor Inlets*, Marine and Freshwater Resources Institute, Victoria, viewed 22 May 2019, <file:///C:/Users/jessf/Downloads/SEAGRASS_MAPPING_OF_VICTORIAS_MINOR_INLETS.pdf>.

Blakey, T Melesse, A & Hall, M 2015, 'Supervised Classification of Benthic Reflectance in Shallow Subtropical Waters Using a Generalized Pixel-Based Classifier across a Time Series', *remote sensing*, vol. 7, no. 5, viewed 11 May 2019, <https://www.researchgate.net/publication/275349751_Supervised_Classification_of_Benthic_Reflectance_in_Shallow_Subtropical_Waters_Using_a_Generalized_Pixel-Based_Classifier_across_a_Time_Series>.

Blaschke, T 2010, 'Object based image analysis for remote sensing', *ISPRS Journal of Photogrammetry and Remote Sensing*, vol. 65, no. 1, viewed 22 March 2019, <https://www.sciencedirect.com/science/article/pii/S0924271609000884>.

Congalton, R 2015, 'Assessing Positional and Thematic Accuracies of Maps Generated from Remotely Sensed Data', in Thenkabail, PS (ed.), *Remotely Sensed Data Characterization, Classification, and Accuracies*, CRC Press LLC, Florence.

Contreras-Silva, A López-Caloca, A Tapia-Silva, O & Cerdeira-Estrada, S 2012, 'Satellite Remote Sensing of Coral Reef Habitats Mapping in Shallow Waters at Banco Chinchorro Reefs, México: A Classification Approach', B Escalante-Ramirez (ed), Remote Sensing – Applications, InTechOpen, London, viewed 22 May 2019, <https://www.researchgate.net/publication/272293192_Satellite_Remote_Sensing_of_Coral_Reef_Habitats_Mapping_in_Shallow_Waters_at_Banco_Chinchorro_Reefs_Mexico_A_Classification_Approach>.

Dekker, A Anstee J & Brando, V 2003, *Seagrass Change Assessment Using Satellite Data for Wallis Lake*, *NSW*, A consultancy report to the Great Lakes Council and Department of Land and Water Conservation, Technical Report, Environmental Remote Sensing Group CSIRO Land and Water Canberra.

Eastman, JR 2001, *Guide to GIS and Image Processing Volume 1*, IDRISI, Worcester, Massachusetts, viewed 2 July 2019, <https://www.mtholyoke.edu/courses/tmillett/course/geog205/files/remote_sensing.pdf>.

EO portal n.d., *Landsat 7*, Website, EO portal, viewed 30 April 2019, <https://directory.eoportal.org/web/eoportal/satellite-missions/l/landsat-7>.

EPA Victoria 2002, *Environmental Condition of Rivers and Streams in the Mitchell, Tambo and Nicholson Catchments*, Publication 853, Information Bulletin, EPA Victoria, Melbourne, viewed 6 October 2019, <https://www.epa.vic.gov.au/~/media/Publications/853.pdf>.

Ferguson, R Korfmacher, K 1997, 'Remote sensing and GIS analysis of seagrass meadows in North Carolina', *Aquatic Botany*, vol. 58, no. 3-4, viewed 22 May 2019 <https://ac.els-cdn.com/S0304377097000387/1-s2.0-S0304377097000387-main.pdf?_tid=d7096efd-77f6-4f4a-bf8c-1adb867cc642&acdnat=1539654315_0e931bff8e2c66d878e79cd83af84f0b>.

Foody, G Mathur, A 2004, 'Toward intelligent training of supervised image classifications: directing training data acquisition for SVM classification', *Remote Sensing of Environment*, vol. 93, viewed 13 May 2019, <https://www.sciencedirect.com/science/article/pii/S003442570400207X>.

Fyfe, S 2003, 'Spatial and temporal variation in spectral reflectance: Are seagrass species spectrally distinct?', *Limnology and Oceanography*, vol. 48, viewed 2 July 2019, <https://pdfs.semanticscholar.org/470d/427779d9c22f3642c16d5df36bb41f4405d1.pdf>.

General Overview 2015, GRASS GIS, Bonn, Germany, viewed 21 May 2019, < https://grass.osgeo.org/documentation/general-overview/>.

Geoscience Australia 2015, *Australian Reflectance Grid 25 (ARG25) Product Desription*, Doc V1.1, Australian Government, Geoscience Australia, Australia, viewed 1 April 2019,

<https://d28rz98at9flks.cloudfront.net/75062/Australian_Reflectance_Grid_ARG25_Product_Description_V1_1.PDF>.

Gippsland Ports 2016, *Map*, Gippsland Ports, Bairnsdale, Victoria, viewed 1 May 2019, <https://www.gippslandports.vic.gov.au/ports-and-waterways/ports-and-waterways/gippsland-lakes/>.

Google Maps Australia 2019, *Satellite Image*, Website, Google, Mountain View, California, viewed 18 May 2019, <https://www.google.ca/maps/@-37.912528,147.8499059,24725m/data=!3m1!1e3>.

Grindgis.com 2016, *Graph*, Website, Grindgis.com, 27 May 2019, <https://grindgis.com/remote-sensing/vegetation-spectral-signature-cheat-sheet>.

Gullan, Walsh & Forbes 1981, 'Vegetation of the Gippsland Lakes Catchment', *National Herbarium*, viewed 22 May 2019, <https://www.rbg.vic.gov.au/documents/Muelleria_4(4),_p333-383,_Gullan_et_al,_Gippsland_Lakes_vegetation.pdf>.

Humboldt State Geospatial Online 2014, *Spectral Reflectance*, Humboldt State University, Arcata, California, viewed 1 July 2019, <http://gsp.humboldt.edu/OLM/Courses/GSP_216_Online/lesson2-1/reflectance.html>.

Intermap Technologies Ltd 2016, *Fundamentals of Remote Sensing*, Tutorial, The Canada Centre for Mapping and Earth Observation, Ottawa, Ontario, viewed 1 July 2019, <https://www.nrcan.gc.ca/sites/www.nrcan.gc.ca/files/earthsciences/pdf/resource/tutor/fundam/pdf/fundamentals_e.pdf>.

Kool, J 2017, *SR-N_25_2.0.0*, Commonwealth of Australia (Geoscience Australia), Symonston, Australian Capital Territory.

Kratochvilova, A Petras, V 2014, *g.gui.iclass*, manual, GRASS GIS, viewed 2 July 2019, <https://grass.osgeo.org/grass72/manuals/g.gui.iclass.html>.

Li, F., Jupp, D, Reddy, S, Lymburner, L, Mueller, N, Tan, P, and Islam, A 2010, 'An Evaluation of the Use of Atmospheric and BRDF Correction to Standardize Landsat Data', *IEEE Journal of Selected Topics in Applied Earth Observations and Remote Sensing*, vol. 3, no. 3, viewed 29 April 2019, <https://www.researchgate.net/publication/224120158_An_Evaluation_of_the_Use_of_Atmospheric_and_BRDF_Correction_to_Standardize_Landsat_Data>.

Li, M Zang, S Zhang, B Li, S & Wu, C 2013, 'A Review of Remote Sensing Image Classification Techniques: the Role of Spatio-contextual Information', *European Journal of Remote Sensing*, vol. 47, no. 1, viewed 10 May 2019, <https://www.tandfonline.com/doi/pdf/10.5721/EuJRS20144723>.

Li, M Zang, S Zhang, B Li, S and Wu C 2014, ‘A Review of Remote Sensing Image Classification Techniques: the Role of Spatio-contextual Information’, *European Journal of Remote Sensing*, vol. 47, no. 1, viewed 23 April 2019, <https://pdfs.semanticscholar.org/a8a7/f187de931c74d50dde47d004bcf427612561.pdf>.

Lyons, M Phinn & Roelfsema C 2010, ‘Long Term Monitoring of Seagrass Distribution in Moreton Bay, Australia, From 1972-2010 Using Landsat MSS, TM, ETM+’, *Conference: Geoscience and Remote Sensing Symposium (IGARSS)*, DOI: 10.1109/IGARSS.2010.5651878.

Lyons, M Phinn, S & Roelfsema C 2012, ‘Long term land cover and seagrass mapping using Landsat and object-based image analysis from 1972 to 2010 in the coastal environment of South East Queensland, Australia’, *ISPRS Journal of Photogrammetry and Remote Sensing*, vol. 71, viewed 20 May 2019,<https://www.sciencedirect.com/science/article/pii/S0924271612000810>.

Lyons, M Roelfsema, C Phinn, S 2013, ‘Towards understanding temporal and spatial dynamics of seagrass landscapes using time-series remote sensing’, *Estuarine, Coastal and Shelf Science*, vol. 120, viewed 7 April 2019, <https://www.sciencedirect.com/science/article/pii/S0272771413000644>.

Maini, A & Agrawal, V 2014, *Satellite Technology: Principles and Applications*, John Wiley & Sons, Incorporated, New York. <https://ebookcentral-proquest-com.ezproxy.usq.edu.au/lib/usq/reader.action?docID=1666477>.

Momsen, E Metz, M 2017, *GRASS GIS manual: i.segment*, Grass Development Team, Bonn, Germany, viewed 28 May 2019, <https://grass.osgeo.org/grass74/manuals/i.segment.html>.

Myint, S Mesev, V Quattrochi, D Wentz, E 2015, ’Urban Image Classification: Per-Pixel Classifiers, Subpixel Analysis, Object-Based Image Analysis, and Geospatial Methods’, in Thenkabail, PS (ed.), *Remotely Sensed Data Characterization, Classification, and Accuracies*, CRC Press LLC, Florence.

New World Encyclopedia 2013, *Benthic zone*, New World Encyclopedia, viewed 1 July 2019, <https://www.newworldencyclopedia.org/entry/Benthic_zone>.

Phinn, S Roelfsema, C n.d., *What is remote sensing?*, toolkit website, Remote Sensing Research Centre, University of Queensland, Brisbane, viewed 12 September 2019, <http://ww2.sees.uq.edu.au/rsrc/rstoolkit/en/html/marine/resources/what-is-remote-sensing.html>.

Roelfsema, C Phinn, S Udy, N Maxwell, P 2009, ‘An integrated field and remote sensing approach for mapping seagrass cover, Moreton Bay, Australia’, *Spatial Science*, vol. 54, no. 1, viewed 11 May 2019,

<https://www.researchgate.net/publication/43511756_An_Integrated_Field_and_Remote_Sensing_Approach_for_Mapping_Seagrass_Cover_Moreton_Bay_Australia>.

Roob, R & Ball, D 1997, *Victorian Marine Habitat Database Gippsland Lakes Seagrass Mapping*, Marine and Freshwater Resources Institute, Victoria, viewed 22 May 2019, <http://www.loveourlakes.net.au/wp-content/uploads/2015/05/Part-A-An-Assessment-of-Seagrass-Changes-in-the-Gippsland-Lakes-Through-a-Review-of-Historic-Aerial-Photographs.pdf>.

Sabins, F 1996, *Remote sensing : principles and interpretation*, 3rd edn, Macmillan Education Australia, New York.

Satellite Imaging Corporation n.d., *WorldView-2 Satellite Sensor*, Houston, Texas, viewed 8 October 2019, <https://www.satimagingcorp.com/satellite-sensors/worldview-2/>.

Shapiro, M Wen, T 2015, *GRASS GIS manual: i.maxlik*, Grass Development Team, Bonn, Germany, viewed 28 May 2019, <https://grass.osgeo.org/grass74/manuals/i.maxlik.html>.

Spectral Signature Cheatsheet – Spectral Bands in Remote Sensing 2018, web document, GIS Geography, viewed 22 May 2019, <https://gisgeography.com/spectral-signature/>.

Smith R 2014, '*GST 105: Introduction to Remote Sensing Lab 6: Accuracy Assessment Objective – Perform an Accuracy Assessment Document*', version 2014-08-11 (Beta), Tutorial, Department of Labor, Washington, District of Columbia, viewed 27 May 2019, <https://foss4geo.files.wordpress.com/2014/08/module-7-lab3.pdf>.

Swinburne University of Technology 2010, *Risk Assessment Template*, Word Document, Hawthorn, Victoria, viewed September 2018, <https://unione.swin.edu.au/files/SSAA/Supplementary-Information/Club%20Off%20Campus%20Event%20Risk%20Assessment%20Form.docx>.

United States Geological Survey n.d., *Landsat 5*, USGS, Reston, Virginia, viewed 30 April 2019, <https://www.usgs.gov/land-resources/nli/landsat/landsat-5?qt-science_support_page_related_con=0#qt-science_support_page_related_con>.

United States Geological Survey n.d., *Landsat 7*, USGS, Reston, Virginia, viewed 30 April 2019, <https://www.usgs.gov/land-resources/nli/landsat/landsat-7?qt-science_support_page_related_con=0#qt-science_support_page_related_con>.

United States Geological Survey n.d., *Landsat Missions*, U.S. Department of the Interior, Washington, District of Columbia, viewed 30 April 2019, <https://www.usgs.gov/land-resources/nli/landsat/landsat-satellite-missions?qt-science_support_page_related_con=2#qt-science_support_page_related_con>.

SVY3202 Photogrammetry & Remote Sensing Module 7, University of Southern Queensland, Toowoomba, viewed 26 April 2019, <http://usqstudydesk.usq.edu.au>.

Van Niel, K Holmes, K Radford, B 2009, *Seagrass Mapping Geographe Bay 2004 – 2007*, Southwest Catchment Council, viewed 22 May 2019, <http://www.web.uwa.edu.au/__data/assets/pdf_file/0006/207465/Seagrass_Mapping04-07_finalx.pdf>.

Veljanovski, T Kanjir, U Oštir, K 2011, 'Object-Based Image Analysis of Remote Sensing Data', *Geodetski Vestnik*, vol. 55, no. 4, viewed 14 May 2019, <https://www.researchgate.net/publication/275607328_Object-based_image_analysis_of_remote_sensing_data>.

Warry, F & Hindell, J 2011, *Fish assemblages and seagrass condition of the Gippsland Lakes: 2011*, Arthur Rylah Institute for Environmental Research, Heidelberg, viewed 14 September 2019, <https://www.loveourlakes.net.au/wp-content/uploads/2015/05/Fish-assemblages-2011.pdf>.

Wulder, M Loveland, T Roy, D Crawford, C Masek, J Woodcock, C Allen, R Anderson, M Belward, A Cohen, W Dwyer, J Erb, A Gao, F Griffiths, P Helder, D Hermosilla, T Hipple, J Hostert, P Hughes, M Huntington, J Johnson, D Kennedy, R Kilic, A Li, Z Lymburner, L McCorkel, J Pahlevan, N Scambos, T Schaaf, C Schott, J Sheng, Y Storey, J Vermote, E Vogelmann, J White, J Wynne, R Zhu, Z 2019, 'Current status of Landsat program, science, and applications', *Remote Sensing of Environment*, vol. 225, viewed 29 April 2019, <https://www.sciencedirect.com/science/article/pii/S0034425719300707>.

Wulder, M Masek, J Cohen, W Loveland, T Woodcock, C 2012, 'Opening the archive: how free data has enabled the science and monitoring promise of Landsat', *Remote Sensing of Environment*, vol. 122, viewed 30 April 2019, <http://citeseerx.ist.psu.edu/viewdoc/download?doi=10.1.1.702.5535&rep=rep1&type=pdf>.

Ye, S Pontius Jr, R Rakshit, R 2018, 'A review of accuracy assessment for object-based image analysis: From per-pixel to per-polygon approaches', *ISPRS Journal of Photogrammetry and Remote Sensing*, vol. 141, viewed 6 May 2019, <https://reader.elsevier.com/reader/sd/pii/S0924271618300947?token=04F3BD0EA7BCC84E913E63B65CDF7092FED59D74C5FF91CEF42DDFBE39D46C4638BE859C953B8C3AFB7FD68ECA255DB7>.

Zaiko, A 2008, *Benthic zone (habitat)*, datasheet, CAB International, Oxfordshire, United Kingdom, viewed 1 July 2019, <https://www.cabi.org/isc/datasheet/107788>.

7.0 Appendix A Project Specification

ENG4111/4112 Research Project

Project Specification

For: Conan Kuzniarski

Title: Remote sensed monitoring of seagrass cover in the Gippsland Lakes, Victoria, Australia.

Major: Surveying

Supervisors: Glenn Campbell

Enrolment: ENG4111 – EXT S1, 2019

ENG4112 – EXT S2, 2019

Project Aim: To establish a cost-effective method for ascertaining the spatial distribution of seagrass meadows in the Gippsland Lakes between 1998 – 2017 using remote sensing.

Programme: Version 2, 15th March 2019

1. Research and review the existing literature.
2. Research the most appropriate software to acquire, to perform pixel-based classifications.
3. Develop rules and methods for pixel-based classification techniques.
4. Use objective measures to determine if a three band or five band combination is more accurate.
5. Apply the most accurate combination to the entire data set to complete the analysis.
6. Draw conclusions on seagrass bed health based on the time series.

If time and resources permit:

7. Compare and/or contrast the results of seagrass meadow extents to that found in previous research, which utilised aerial photography methods.
8. Investigating spatial changes of seagrass meadows due to significant events such as flooding.